

2 **Synthesis, Spectral and Thermal Characterization**
3 **with Antimicrobial Activity Studies on Some Metal**
4 **Complexes Containing Schiff Base Ligand**
5
6
7

8 Abstract

9 Some metal complexes of Ni(II), Zn(II), Mn(II), Sn(II), Co(II) and Cd(II) ions were
10 synthesized with three different synthesized Schiff base ligands. The ligands and metal
11 complexes were isolated in solid state from the reaction medium and characterized by molar
12 conductivity measurement, magnetic susceptibility, Infrared, electronic spectral, thermal
13 analysis and some physical measurements. The overall reactions were monitored by TLC
14 analysis. Molar conductance study have shown that all the complexes were non electrolytic in
15 nature. FTIR studies suggested that Schiff bases act as deprotonated bidentate ligands and
16 metal ions are attached with the ligands through N, O/S coordinating sites during
17 complexation reaction. Magnetic susceptibility data coupled with electronic spectra revealed
18 that Zn(II), Mn(II), Sn(II), and Cd(II) complexes have tetrahedral, Ni(II) complexes has square
19 planer and Co(II) complexes has octahedral geometry. Thermal analysis (TGA and DTG) data
20 showed the possible degradation pathway of the complexes and also indicated that most of
21 the complexes were thermally stable up to 200⁰C. The Schiff bases and their metal complexes
22 have been found moderate to strong antimicrobial activity.

23 Keywords: Schiff Base, Thiosemicarbazide, TGA, DTG, Antimicrobial activity

24 **1 INTRODUCTION**

25 Multidentate ligands are extensively used for the preparation of metal complexes with
26 interesting properties [1-5]. Among these ligands, Schiff bases containing nitrogen and
27 phenolic oxygen donor atoms are of considerable interest due to their potential application in
28 catalysis, medicine and material science [6-9]. Transition metal complexes of these ligands
29 exhibit varying configurations, structural liability and sensitivity to molecular environments.
30 The central metal ions in these complexes act as active sites for pharmacological agent.
31 This feature is employed for modeling active sites in biological systems.

32 Thiosemicarbazones obtained by the condensation reaction of thiosemicarbazide and
33 different aldehydes or ketones are important chemicals due to their broad profile of
34 pharmacological activity. The transition metal complexes of thiosemicarbazone are also
35 played important role in antimicrobial, antitumor and anticancer activities.

36 Therefore, in view of our interest in synthesis of new Schiff base complexes, which might
37 find application as pharmacological and as luminescence probes, we have synthesized and
38 characterized new transition metal complexes of Schiff bases formed by the condensation
39 reaction of different aldehydes and amino acids. The results of our studies are presented in
40 this article.

41 **2. Experimental**

42 **2.1 Materials and Methods**

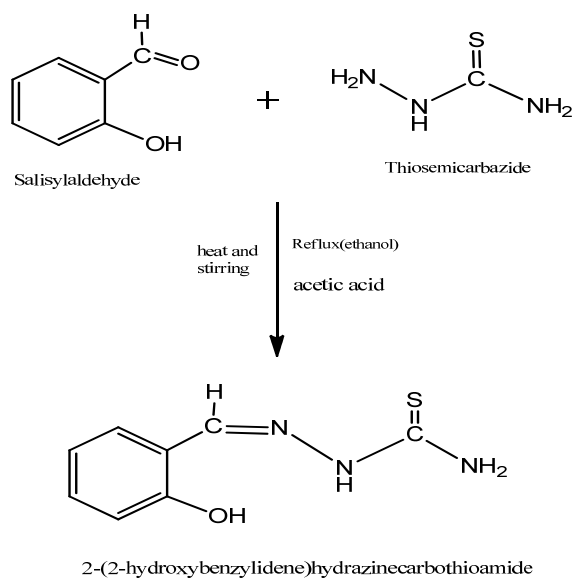
43 All chemicals and solvents used were of Analar grade. All metal(II) salts were used as
44 chloride and sulphate. The solvents such as Ethanol, methanol, chloroform, Diethyl ether,
45 petroleum ether, DMSO (dimethyl sulfoxide) and acetonitrile were purified by standard
46 procedure. The melting point or the decomposition temperature of all the prepared ligand and
47 metal complexes were observed in an electro thermal melting point apparatus model No.
48 AZ6512. Vibrational spectra (IR) were recorded with a NICOLET 310, FTIR
49 spectrophotometer, Belgium, in the range $4000-225\text{ cm}^{-1}$ with a KBr disc as reference. UV-
50 Visible spectra of the complexes in DMSO ($0.5 \times 10^{-3}\text{ M}$) were recorded in the region 200-800
51 nm on a Thermoelectron Nicolet evolution 300 UV-Visible spectrophotometer. The
52 SHERWOOD SCIENTIFIC Magnetic Susceptibility Balance that following the Gouy
53 Method were used to measure the magnetic moment of the solid complexes. The electrical
54 conductance measurements were made at room temperature in freshly prepared aqueous
55 solution (10^{-3} M) and in DMSO using a WPACM35 conductivity meter and a dip-cell with a
56 platinum electrode. The thermogravimetric analyses (TGA) were performed on Perkin Elmer
57 Simultaneous Thermal Analyzer, STA-8000. The purity of the ligand and metal complexes
58 were tested by Thin Layer Chromatography (TLC).

59

60 **2.1 Synthesis of Schiff base Ligand $\text{C}_8\text{H}_9\text{ON}_3\text{S}$ (L^1)**

61 The ligand was prepared by condensation reaction of 20 mmole of salicylaldehyde (1.048ml)
62 with 20 mmole (1.82gm) of thiosemicarbazide in a clean round bottomed flask.
63 Salicylaldehyde was dissolved in 20ml ethanol and thiosemicarbazide was dissolved in hot

64 ethanol with water. The solutions were mixed and refluxed for 3-4 hours. On cooling off
65 white colored product was formed which was washed with ethanol, acetone, and diethyl ether
66 and dried in vacuum desiccators over anhydrous CaCl_2 . The purity of ligand was tested by
67 TLC using different solvents. The product was found to be soluble in methanol, chloroform
68 and DMSO. It provided 80% yield at 34°C . The target Schiff base was synthesized according
69 to Schema-1.

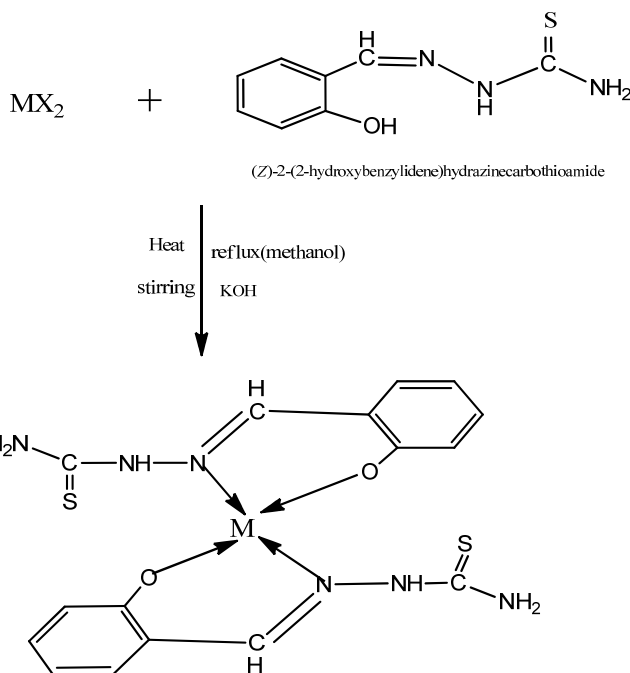


70

71 Schema 1: Synthetic pathway of Schiff base ligand $\text{C}_{14}\text{H}_{11}\text{O}_3\text{N}$ (L^1)

72 2.3 Synthesis of Metal Complexes Using Schiff Base Ligand $\text{C}_{14}\text{H}_{11}\text{O}_3\text{N}$ (L^1)

73 The synthesized complexes have the general formula $[\text{M}(\text{SB})_2]$; where $\text{M} = \text{Zn}(\text{II}), \text{Ni}(\text{II})$ and
74 $\text{Mn}(\text{II})$ and $\text{SB} =$ synthesized Schiff base ligand (Schema 2). During complexation
75 reaction, 15ml methanolic solution of Zinc(II) sulphate (0.2875g, 1mmol)/ Ni(II) chloride
76 hexahydrate (0.238g, 1mmol)/ Manganese(II) chloride tetrahydrate (0.198g, 1mmol) was
77 taken in a two necked round bottom flask and kept on a magnetic stirring. A methanolic
78 solution (20 mL) of prepared Schiff base ligand (0.390g, 2mmol) was added drop wise and a
79 methanolic solution (10mL) of KOH (0.1122g, 1mmol) was added slowly then the resultant
80 mixture was heated with constant stirring on a magnetic stirrer for 4-5 hours. On cooling
81 colored solid product was formed which was washed with methanol, acetone, ether and dried
82 in vacuum over anhydrous CaCl_2 . The reaction was monitored by TLC using petroleum ether,
83 toluene, ethyl acetate and methanol as solvent. The common structure of metal complexes has
84 been shown in Schema-1 and individual expected structures of the complexes are shown as
85 supplementary materials.



86

87

Schema 2: Synthetic pathway of Schiff Base Ligand (L^2) Metal Complexes

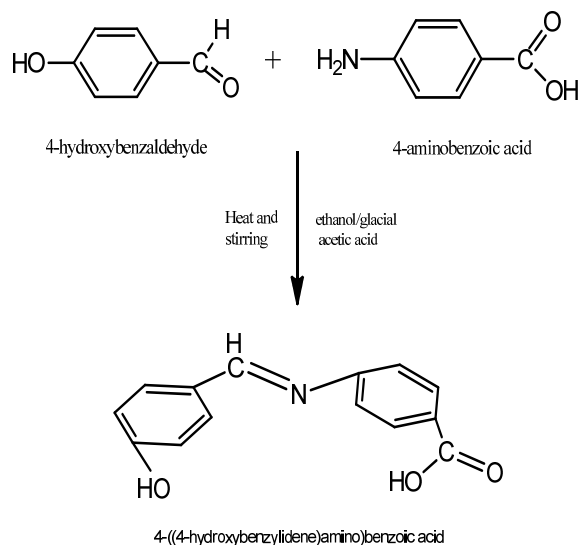
88

Where, $M = \text{Zn(II)}$, Ni(II) , Mn(II) , and Sn(II) ions and $X = \text{Cl}^-$, SO_4^{2-} ions

89

90 2.4 Synthesis of Schiff Base Ligand $\text{C}_{14}\text{H}_{11}\text{O}_3\text{N}$ (L^2)

91 4-hydroxy benzaldehyde (2.44g, 20 mmol) dissolved in absolute ethanol (20-25 mL) was
 92 added dropwise to a constant stirring solution of 4-aminobenzoic acid(2.76 g, 20 mmol) in 30
 93 mL ethanol and 2 mL of conc. glacial acetic acid was added slowly. Then the mixture was
 94 refluxed for (4-5)h. On cooling, a solid yellow product was formed which was filtered,
 95 washed with ethanol and diethyl ether and dried in vacuum over anhydrous CaCl_2 . The
 96 reaction was monitored by TLC using petroleum ether, ethyl acetate, toluene and methanol
 97 solvents. The product was found to be soluble in methanol, chloroform and DMSO. It
 98 provided 65% yield at 34°C . The target Schiff base was synthesized according to Schema-3.



99

100

Schema-3: Synthetic pathway of Schiff base ligand $C_{14}H_{11}O_3N$ (L^2)

101

2.5 Synthesis of Metal Complex Using Schiff Base Ligand (L^2)

102

The complex was prepared in 1:2 molar ratio (metal : ligand). A methanolic solution (20

103

mL) of cobalt(II) chloride hexahydrate (0.24 g, 1 mmol)) was taken in a two necked round

104

bottom flask and kept on magnetic stirring and a methanolic solution (20 mL) of prepared

105

Schiff base ligand (0.483 g, 2 mol) was added dropwise and stirred with heating for 4-5h. On

106

cooling, precipitate was formed which was filtered, washed with ethanol, acetone, and diethyl

107

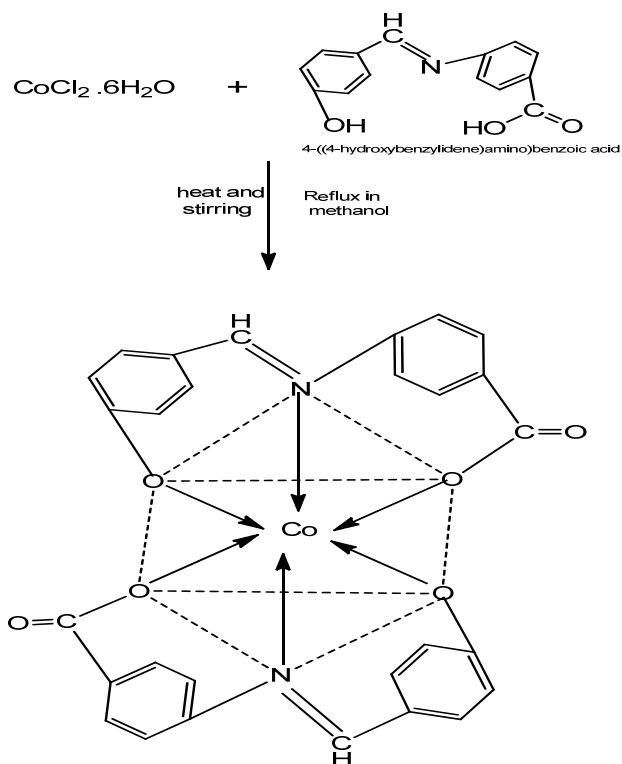
ether and dried in vacuum desiccators over anhydrous $CaCl_2$. The purity of complex was

108

tested by TLC using different solvents. The complex was soluble in DMSO with heat. The

109

proposed structure of complex is shown in Schema-4.

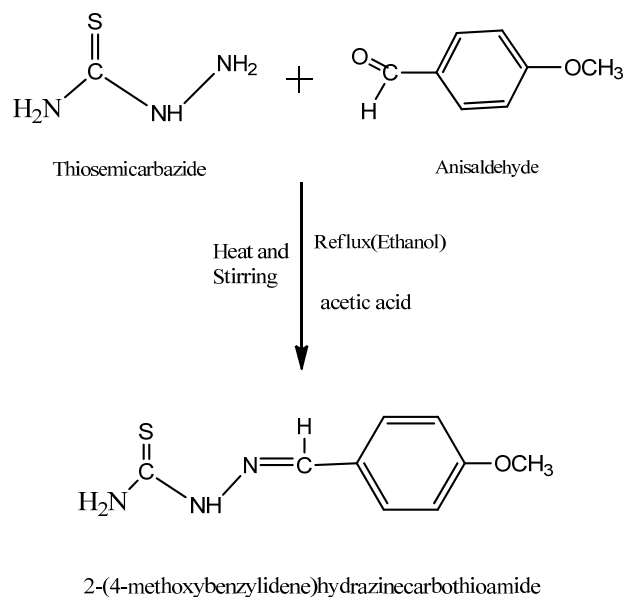


110

111 Schema-4: Synthetic pathway of Co(II) complex with Schiff Base Ligand (L^2)

112 **2.6 Synthesis of Schiff base Ligand $C_9H_{11}N_3OS$ (L^3)**

113 To a stirring solution of thiosemicarbazide (0.91 gm, 10 mmol) dissolved in 20mL of ethanol
 114 with water, a solution of Anisaldehyde(1.22mL,10mmol) in 10mL ethanol was added dropwise.
 115 After sometime 2ml of glacial acetic acid was added with the reaction mixture and the solution
 116 was refluxed for 5-6 h and allowed to cool overnight in room temperature. The off white
 117 product was filtered washed several times with ethanol and finally with diethyl ether and dried in
 118 vacuum over anhydrous CaCl_2 . The reaction was monitored by TLC using petroleum ether,
 119 ethyl acetate, toluene and methanol solvents .The product was found to be soluble in methanol,
 120 DMF and DMSO. It provided 62% yield. The Schiff base was synthesized according to
 121 Schema-5.



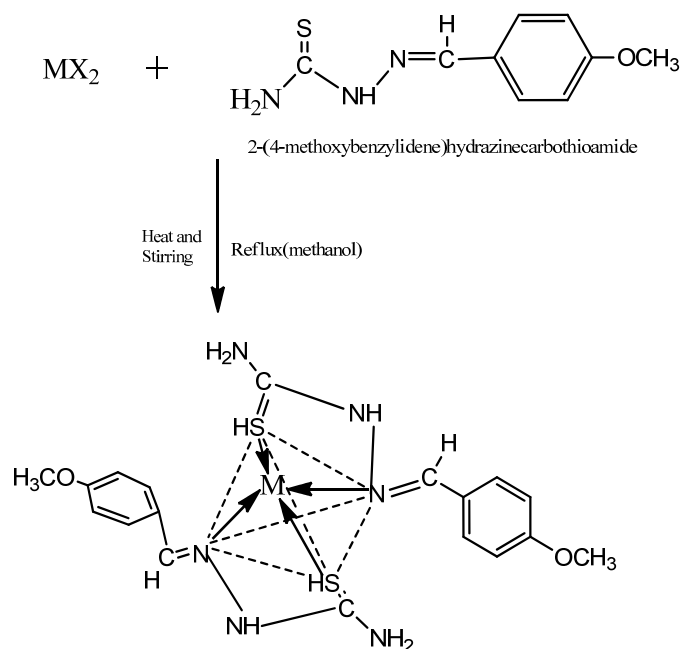
122

123

Schema-5: Synthetic pathway of Schiff base ligand $C_9H_{11}N_3OS$ (L^3)

124 **2.7 Synthesis of Metal Complex Using Schiff Base Ligand (L^3):**

125 The complex was prepared in 1:2 molar ratio (metal : ligand). Methanolic solution (20 mL) of
 126 cadmium(II) chloride dihydrate (0.228g, 1mmol) was taken in a two necked round bottom
 127 flask and kept on magnetic stirring. A methanolic solution (20 mL) of prepared Schiff base
 128 ligand (L^3) (0.418g, 2mmol) was added dropwise and stirred with heating for 4-5h. On
 129 cooling, precipitate was formed which was filtered, washed with ethanol, acetone, and diethyl
 130 ether and dried in vacuum desiccators over anhydrous $CaCl_2$. The reaction was monitored by
 131 TLC using different solvents. The complex was soluble in DMSO with heat. The proposed
 132 structure of complex is shown in Schema-6.



133

134 Schema-6: Synthetic pathway of Schiff Base Ligand (L^4) Metal Complex

135

Where, $M=Cd(II)$ ions

136 3. Characterization of the Ligands and Complexes

137 The structures of the complexes were characterized by melting point, conductivity
 138 measurements, magnetic susceptibility, IR spectra and UV visible spectra [10] analysis. The
 139 purity of the ligands and metal complexes were monitored by Thin Layer Chromatography
 140 (TLC). The ligands and complexes are characterized below by these methods.

141

142 3.1 Melting point

143 Melting point gives an approximate idea about the nature of the complexes and can suggest
 144 whether it is covalent or ionic [11]. The melting point of all the synthesized ligands and
 145 complexes are shown in Table-1.

146

147 **Table-1:** Physical characteristics and analytical data of ligands and complexes

Compound/Empirical Formula	Formula Weight	Color	Yield(%)	Melting Point/ Decomposition temp.($^{\circ}C$)
Ligand (L^1) $C_8H_9ON_3S$	195	off white	80 %	215 $^{\circ}C$ - 217 $^{\circ}C$

[Zn (L ¹) ₂].2H ₂ O [ZnC ₁₆ H ₁₆ O ₂ N ₆ S ₂].2H ₂ O	491.38	cream color	67 %	above 300 ⁰ C
[Ni (L ¹) ₂].H ₂ O [NiC ₁₆ H ₁₆ O ₂ N ₆ S ₂].H ₂ O	466.93	yellow green	70 %	275 ⁰ C - 280 ⁰ C
[Mn (L ¹) ₂].H ₂ O [MnC ₁₆ H ₁₆ O ₂ N ₆ S ₂].H ₂ O	462.94	golden rod	65 %	275 ⁰ C - 280 ⁰ C
[Sn (L ¹) ₂] [SnC ₁₆ H ₁₆ O ₂ N ₆ S ₂]	508.71	greenish yellow	60%	240 ⁰ C - 250 ⁰ C
Ligand (L ²) C ₁₄ H ₁₁ O ₃ N	241	yellow	65 %	241 ⁰ C - 245 ⁰ C
[Co(L ²) ₂].2H ₂ O [CoC ₂₈ H ₁₈ O ₆ N ₂].2H ₂ O	576.93	golden rod	56 %	above 300 ⁰ C
Ligand (L ³) C ₉ H ₁₁ N ₃ OS	209	off white	62%	145 ⁰ C - 150 ⁰ C
[Cd(L ³) ₂] [CdC ₁₈ H ₂₂ O ₂ N ₆ S ₂]	530.41	white	75 %	260 ⁰ C - 265 ⁰ C

148

149 3.2 Characterizations by Conductivity

150

151 The molar conductivities were obtained using the formula

$$152 \quad \Lambda = \frac{1000}{C} \times \text{Cell constant} \times \text{Observed conductivity.}$$

153 Where, Λ =molar conductance

154 C= concentration

155 The molar conductance is calculated from the measured specific conductance at room
156 temperature by using the above equation. The experimental results are shown in Table-2.

157

158 **Table-2:** Data for the determination of Molar conductivity

Name of Complex	Observed conductivity	Molar conductance	μ_{eff} in B.M.	No. of unpaired electron
-----------------	-----------------------	-------------------	----------------------------	--------------------------

	(ohm ⁻¹ cm ² mol ⁻¹)	Λ = (1000/c) × specific conductance Scm ² mol ⁻¹		
[Zn (L ¹) ₂].2H ₂ O [ZnC ₁₆ H ₁₆ O ₂ N ₆ S ₂].2H ₂ O	3	3	0.567	–
[Ni (L ¹) ₂].H ₂ O [NiC ₁₆ H ₁₆ O ₂ N ₆ S ₂].H ₂ O	6	6	1.471	–
[Mn (L ¹) ₂].H ₂ O [MnC ₁₆ H ₁₆ O ₂ N ₆ S ₂].H ₂ O	8	8	2.576	1
[Sn (L ¹) ₂] [SnC ₁₆ H ₁₆ O ₂ N ₆ S ₂]	9	9	0.639	–
[Co(L ²) ₂].2H ₂ O [CoC ₂₈ H ₁₈ O ₆ N ₂].2H ₂ O	8	8	4.017	3
[Cd(L ³) ₂] [CdC ₁₈ H ₂₂ O ₂ N ₆ S ₂]	6	6	0.461	–

159

160 From the above table data it is showed that all the complexes are non-electrolyte.

161 3.3 Characterizations by Magnetic Susceptibility

162 **Measurement of magnetic susceptibility:** The measurements of magnetic susceptibilities
163 were made at about constant temperature; Curie-law was used and was calculated from the
164 equation.

$$165 \mu_{\text{eff}} = 2.83 \sqrt{\chi_m^{\text{corr}} \cdot T} \text{ B.M.}$$

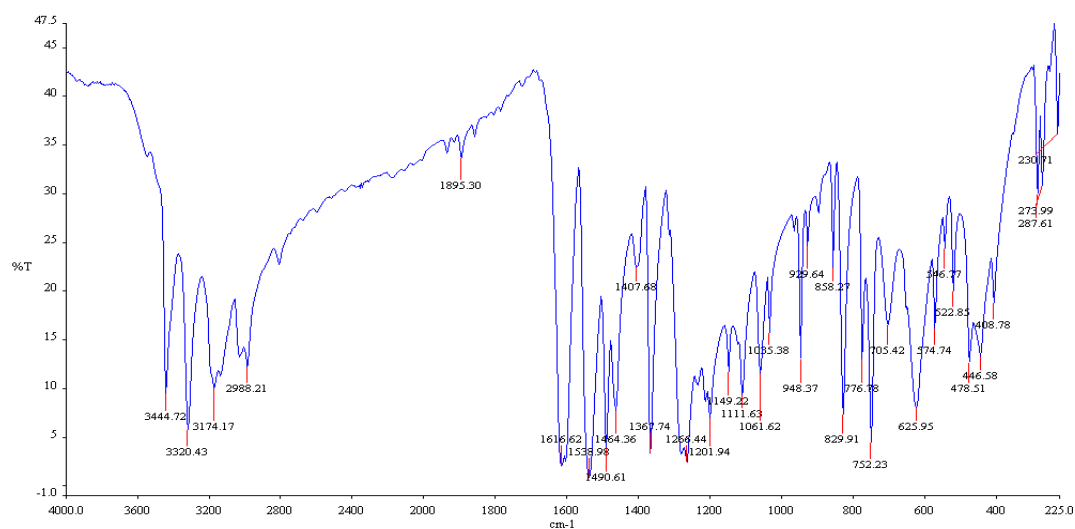
166 Thus μ_{eff} obtained is known as effective magnetic moment. All the values and weight were
167 expressed in C.G.S. units. The observed values of effective magnetic moment (μ_{eff}) of the
168 complexes at room temperature are given in table 2. From the above data it is showed that the
169 Zn(II), Ni(II), Sn(II) and Cd(II) ions complexes are diamagnetic and Mn(II) and Co(II) ions
170 complexes are paramagnetic in nature[13].

171 **3.4 Measurement of IR spectra:** At first the complexes heat six hour and KBr overnight in oven.
172 Then the complexes and KBr grind with pestle in mortar. Infrared spectra disc were recorded as
173 KBr with a NICOLET 310, FTIR spectrophotometer, Belgium, from 4000-225 cm⁻¹.

174 3.4.1 IR spectra of Schiff Base ligand C₈H₉ON₃S (L¹) and It's metal complexes

175 **a. IR spectra of Schiff Base ligand C₈H₉ON₃S (L¹)**

176 The spectrum of ligand showed a strong absorption band at 1616 cm⁻¹ due to the azomethine
177 $\nu(\text{C}=\text{N})$ stretching frequency of the free ligand [14-18] indicating that the condensation have
178 taken place between the CHO moiety of salicylaldehyde and -NH₂ moiety of
179 thiosemicarbazide. The IR spectra of the free ligand (figure-1) showed two bands at 3320 cm⁻¹
180 and 3174 cm⁻¹ may be attributed to the free -NH₂ and $\nu(\text{N}-\text{H})$ groups respectively. These
181 bands remains in the same region in all complexes spectra, suggesting nonparticipation in
182 coordination of one terminal -NH₂ group in thiosemicarbazone [15,19-21] The band
183 observed at 3444 cm⁻¹ was assigned to the $\nu(\text{O}-\text{H})$ of hydroxyl group [14,15,22]. The strong
184 band 776 cm⁻¹ for $\nu(\text{C}=\text{S})$ indicated that C=S bond was present in the Schiff base ligand
185 [14,22].



186

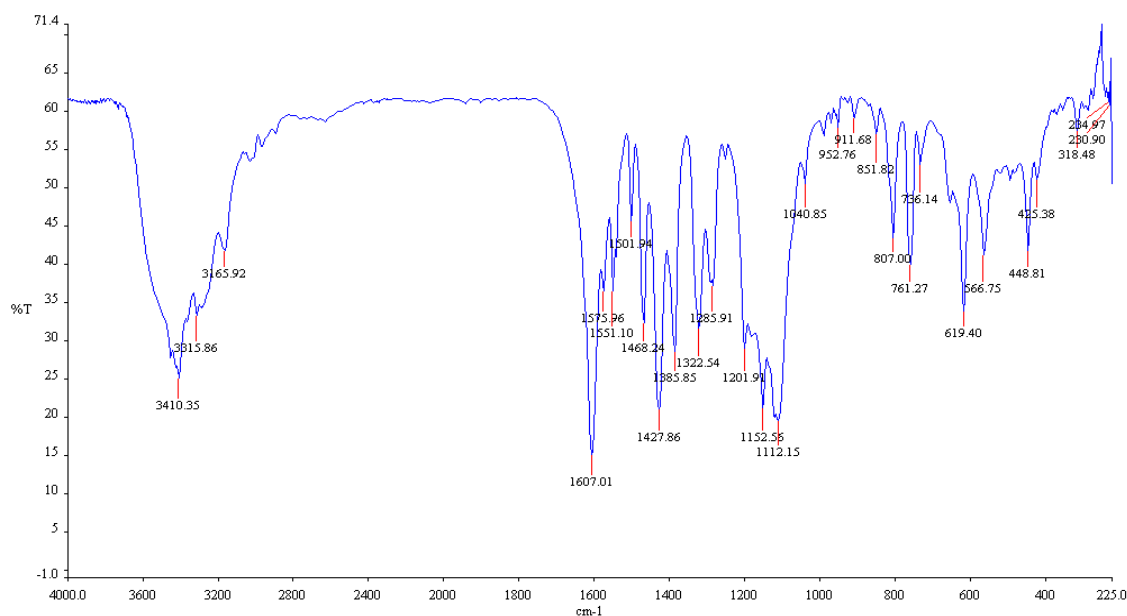
187 Figure-1: IR spectra of Schiff base ligand C₈H₉ON₃S (L¹)

187

188 **b. IR spectra of [ZnC₁₆H₁₆O₂N₆S₂].2H₂O complex**

189 In order to determine the mode of coordination of ligand to metal in complexes, IR spectrum
190 of ligand was compared with IR spectrum of metal complexes (figure-2). The band at 1616
191 cm⁻¹ due to the azomethine $\nu(\text{C}=\text{N})$ stretching frequency of the free ligand that shifted to
192 lower frequency in the spectra of the Zn (II) complex at 1607 cm⁻¹ which indicated the
193 coordination through azomethine N atom. The band 3444 cm⁻¹ due to the $\nu(\text{O}-\text{H})$ of hydroxyl
194 group in the IR spectra of the ligand was absent and shifted to lower absorption frequency in
195 the IR spectra of Ni(II) complex indicated the coordination through the phenolic oxygen
196 [23,24]. This is confirmed by the shift of $\nu(\text{C}-\text{O})$ stretching vibration observed at 1266cm⁻¹ in
197 the spectra of free ligand to 1285 cm⁻¹ stretching vibration of complex after coordination

198 [16], which corresponds to forming of weaker C-O(Zn) bond comparing to C-O(H) and
 199 confirms coordination of ligand to Ni(II) via deprotonated phenolic oxygen [25,26]. Also the
 200 medium intensity bands observed at 566 cm⁻¹ is attributed to M-O and 448 cm⁻¹ is attributed
 201 to M-N bonds [27]. IR spectral components of the synthesized complexes are shown in Table
 202 – 3.



203

Figure-2: IR spectra of [ZnC₁₆H₁₆O₂N₆S₂].2H₂O complex

204

205 **Table-3:** FTIR spectral data of the ligand C₈H₉ON₃S (L¹) and it's metal complexes (in cm⁻¹)

Ligand / Metal Complexes	IR/cm ⁻¹				
	ν(O-H)	ν(C=N)	ν(C-O)	ν(M-O)	ν(M-N)
C ₈ H ₉ ON ₃ S	3444	1616	1266	-	-
[ZnC ₁₆ H ₁₆ O ₂ N ₆ S ₂].2H ₂ O	3410	1607	1285	566	448
[NiC ₁₆ H ₁₆ O ₂ N ₆ S ₂].H ₂ O	3412	1607	1294	567	457
[MnC ₁₆ H ₁₆ O ₂ N ₆ S ₂].H ₂ O	3413	1600	1296	570	442
[SnC ₁₆ H ₁₆ O ₂ N ₆ S ₂]	3436	1610	1286	594	458

206

207 **3.4.2 IR spectra of Schiff Base ligand C₁₄H₁₁O₃N (L²) and It's metal complex**

208 **a. IR spectra of Schiff Base ligand C₁₄H₁₁O₃N (L²)**

209 The bands at 1735 cm⁻¹ and 3420 cm⁻¹ due to carbonyl (C=O) and NH₂ stretching vibrations
210 of the starting reagents respectively were absent in the spectra of ligand and a strong new
211 band at 1620 cm⁻¹ was appeared which assigned to the azomethine (HC=N) linkage, a
212 fundamental feature of Schiff base ligand [28,29]. This indicated that amino and aldehyde
213 moieties of the starting reagents have been converted into the azomethine moiety. The bands
214 at 1320 cm⁻¹ due to ν(C-O) of phenolic group and 3410 cm⁻¹ due to the phenolic ν(OH) were
215 also observed in the spectra of ligand [23]. The bands at 1680 cm⁻¹ due to ν(C=O) stretching
216 vibration and 3080 cm⁻¹ due to carboxylic – ν(OH) were observed in the IR spectra of ligand
217 [30-33].

218

219 **b. IR Spectra of [CoC₂₈H₁₈O₆N₂].2H₂O**

220 The band at 1620 cm⁻¹ due to the azomethine –HC=N stretching vibration was shifted to
221 lower frequency at 1541 cm⁻¹ in the metal complex compared to free ligand, suggested the
222 coordination of metal ion through nitrogen of azomethine group [34-36]. The N atom of
223 azomethine would reduce the electron density in the azomethine link and thus lower the –
224 HC=N absorption after coordination. This is further substantiate by the presence of a new
225 band at 457 cm⁻¹ assignable to ν(M-N). The disappearance of phenolic ν(OH) band at 3410
226 cm⁻¹ in Co(II) complex suggested the co-ordination by the phenolic oxygen after
227 deprotonation to the metal ions. This is further supported by shifting of ν(C-O) phenolic
228 band at 1320 cm⁻¹ to lower wave number at 1305 cm⁻¹ in the metal complex. The appearance
229 of a new band at 590cm⁻¹ due to ν(M-O) in the Co(II) complex which further substantiate .
230 The band at 1680 cm⁻¹ assigned to ν(C=O) in the spectra of ligand also shifted to lower
231 frequency range in the metal complex. That suggested the involvement of oxygen atom of
232 carboxylic ν(-OH) group to the coordination with metal ions. The comparison of the IR
233 spectra of the Schiff base and it's metal chelates indicated that the Schiff base ligand
234 coordinated to metal ions by three donor atoms representing the ligand acting in a tri-
235 dentative manner. Spectral data of [CoC₂₈H₁₈O₆N₂].2H₂O is shown in Table 4.

236 **c. IR spectra of [NiC₁₆H₁₆O₂N₆S₂].H₂O complex**

237 In order to determine the mode of coordination of ligand to metal in complexes IR spectrum
238 of ligand was compared with IR spectrum of metal complexes [14, 23]. The band at 1616 cm⁻¹

239 ¹ due to the azomethine $\nu(\text{C}=\text{N})$ stretching frequency of the free ligand that shifted to lower
240 frequency in the spectra of the Ni(II) complex (figure-13) at 1607cm^{-1} indicating the
241 coordination through N atom [5-9]. The band 3444cm^{-1} due to the $\nu(\text{O}-\text{H})$ of hydroxyl
242 group in the IR spectra of the ligand was absent and shifted to lower absorption frequency in
243 the IR spectra of Ni(II) complex indicated the coordination through the phenolic oxygen
244 [22,24]. This is confirmed by the shift of $\nu(\text{C}-\text{O})$ stretching vibration observed at 1266cm^{-1}
245 in the spectra of free ligand to 1294cm^{-1} stretching vibration of complex after coordination
246 [16], which corresponds to forming of weaker C-O(Ni) bond comparing to C-O(H) and
247 confirms coordination of ligand to Ni(II) via deprotonated phenolic oxygen. Also the medium
248 intensity bands observed at 567cm^{-1} is attributed to M-O and 457cm^{-1} is attributed to M-N
249 bonds [27].

250 **d. IR spectra of $[\text{MnC}_{16}\text{H}_{16}\text{O}_2\text{N}_6\text{S}_2]$**

251 The band at 1616cm^{-1} due to the azomethine $\nu(\text{C}=\text{N})$ stretching frequency of the free ligand
252 that shifted to lower frequency in the spectra of the Mn(II) complex at 1600cm^{-1} indicating
253 the coordination through N atom. The band 3444cm^{-1} due to the $\nu(\text{O}-\text{H})$ of hydroxyl group
254 in the IR spectra of the ligand was absent and shifted to lower absorption frequency in the IR
255 spectra of Mn(II) complex indicated the coordination through the phenolic oxygen. This is
256 confirmed by the shift of $\nu(\text{C}-\text{O})$ stretching vibration observed at 1266cm^{-1} in the spectra of
257 free ligand to 1296cm^{-1} stretching vibration of complex after coordination, which
258 corresponds to forming of weaker C-O(Mn) bond comparing to C-O(H) and confirms
259 coordination of ligand to Mn(II) via deprotonated phenolic oxygen [5,17]. Also the medium
260 intensity bands observed at 570cm^{-1} is attributed to M-O and 442cm^{-1} is attributed to M-N
261 bonds [27].

262 **e. IR spectra of $[\text{SnC}_{16}\text{H}_{16}\text{O}_2\text{N}_6\text{S}_2]$**

263 The band at 1616cm^{-1} due to the azomethine $\nu(\text{C}=\text{N})$ stretching frequency of the free ligand
264 that shifted to lower frequency in the spectra of the Sn(II) complex at 1610cm^{-1} indicating
265 the coordination through N atom. The band 3444cm^{-1} due to the $\nu(\text{O}-\text{H})$ of hydroxyl group in
266 the IR spectra of the ligand was absent and shifted to lower absorption frequency in the IR
267 spectra of Sn(II) complex indicated the coordination through the phenolic oxygen. This is
268 confirmed by the shift of $\nu(\text{C}-\text{O})$ stretching vibration observed at 1266cm^{-1} in the spectra of
269 free ligand to 1286cm^{-1} stretching vibration of complex after coordination, which
270 corresponds to forming of weaker C-O(Sn) bond comparing to C-O(H) and confirms

271 coordination of ligand to Sn(II) via deprotonated phenolic oxygen . Also the medium
 272 intensity bands observed at 594cm⁻¹ is attributed to M-O and 458cm⁻¹ is attributed to M-N
 273 bonds.

274

275 **Table-4:** FTIR spectral data of the ligand L² and [CoC₂₈H₁₈O₆N₂].2H₂O (in cm⁻¹)

Ligand / Metal Complexes	IR/cm ⁻¹					
	ν(O-H)	ν(C=N)	ν(C=O)	ν(C-O)	ν(M-O)	ν(M-N)
C ₁₄ H ₁₁ O ₃ N	3410	1620	1680	1320	-	-
[CoC ₂₈ H ₁₈ O ₆ N ₂].2H ₂ O	3436	1541	1598	1305	590	457

276

277 **3.4.3 IR spectra of Schiff Base ligand C₉H₁₁N₃OS (L³) and It's metal complex**

278 **a. IR-Spectra of Schiff base C₉H₁₁N₃OS (L³)**

279 The peaks obtained at 3406cm⁻¹ and 3291cm⁻¹ may be assigned to symmetric and asymmetric
 280 ν(-N-H) stretching frequency of primary amino group. The broad peak obtained between
 281 3282 and 2829 cm⁻¹ may be assigned to overlapping of peaks of hydrogen bonded ν(N-H)
 282 and aromatic C-H stretching frequency. The bands obtained between 1183 cm⁻¹ and 1252 cm⁻¹
 283 in ligand were due to ν(-OCH₃) groups (Table-5). The peaks observed at 1606 cm⁻¹ and 834
 284 cm⁻¹ may be assigned to ν(C=N) and ν(C=S) [37-39].

285 **b. IR-Spectra of [C₁₈H₂₂CdO₂N₆S₂] with ligand (L³)**

286 The bands at 1606 cm⁻¹ and 834 cm⁻¹ assigned to ν(C=N) and ν(C=S) modes and these bands
 287 shifted towards lower frequency in the spectra of Cd(II) complex (Table-5), which indicated
 288 that coordination takes place through nitrogen of ν(C=N) group and sulphur of ν(C=S) group.
 289 At lower frequency the complex exhibited new bands at 540 and 397 cm⁻¹ which further
 290 supported the coordination site ν(M-N) and ν(M-S) vibrations.

291

292 **Table-5:** FTIR spectral data of the ligand L³ and its Cd(II) metal complex (in cm⁻¹)

Ligand / Metal	IR/cm ⁻¹
----------------	---------------------

Complexes	$\nu(\text{C}=\text{N})$	$\nu(\text{C}=\text{S})$	$\nu(\text{M}-\text{N})$	$\nu(\text{M}-\text{S})$
Ligand (L^3) $\text{C}_9\text{H}_{11}\text{N}_3\text{OS}$	1606	834	-	-
$[\text{Cd}(\text{L}^3)_2]$ $[\text{CdC}_{18}\text{H}_{22}\text{O}_2\text{N}_6\text{S}_2]$	1574	821	528	397

293

294 3.5 Characterization by UV-visible Spectra

295 a. UV-vis spectra and magnetic moment of Zn(II) complex with ligand $\text{C}_8\text{H}_9\text{ON}_3\text{S}$ (L^1)

296 The electronic spectral data for the ligand and their metal complex recorded in DMSO are
 297 summarized in Table-6. There are two absorption bands, assigned to $n-\pi^*$ and $\pi-\pi^*$
 298 transitions, in the electronic spectrum of the ligand. These transitions are also found in the
 299 spectra of the complexes, but they are shifted towards lower and higher frequencies,
 300 indicating the coordination of the ligand to the metallic ions [40]. The UV spectra of the
 301 ligand shows three absorption bands at 260nm,310nm and 355nm.The first two bands are
 302 assigned to $\pi-\pi^*$ transitions of azomethine chromospheres and a benzene ring and the third is
 303 assigned to $n-\pi^*$ transition of a lone pair of electrons of an azomethine nitrogen and an
 304 antibonding π orbital. The absorption band $n-\pi^*$ at 355 nm due to an imine group in the
 305 ligand, whereas for the zinc complex, the same was observed at 390 nm with weak absorption
 306 intensity which indicate the coordination of zinc with imine group [41]. The zinc complex
 307 shows only the charge transfer transition which can be assigned to charge transfer from the
 308 ligand to the metal and vice versa, no d-d transitions are expected for $d^{10}\text{Zn}(\text{II})$ complex [42].

309 b. UV-vis spectra and magnetic moment of Ni(II) complex with ligand $\text{C}_8\text{H}_9\text{ON}_3\text{S}$ (L^1)

310 The UV-Vis absorption spectra of the ligand and complex were recorded after dissolving into
 311 DMSO solvent at room temperature. There are two absorption bands, assigned to $n-\pi^*$ and
 312 $\pi-\pi^*$ transitions, in the electronic spectrum of the ligand. These transitions are also found in
 313 the spectra of the complexes, but they are shifted towards lower and higher frequencies,
 314 confirming the coordination of the ligand to the metallic ions [43]. The electronic spectrum of
 315 ligand exhibits three intense absorption peaks at 260 nm, 310 nm and 350nm.The first and
 316 second peaks were attributed to benzene $\pi-\pi^*$ and imino $\pi-\pi^*$ transitions and the third peak in
 317 the spectra was assigned to $n-\pi^*$ transition [44]. The electronic spectra of the Ni(II) complex
 318 with an electronic configuration of d^8 shows three new absorption bands in the visible region

319 and these three bands of the transitions ${}^1A_{1g} \rightarrow {}^1A_{2g}$ (355nm), ${}^1A_{1g} \rightarrow {}^1B_{1g}$ (380nm) and
320 ${}^1A_{1g} \rightarrow {}^1E_g$ (420 nm) were observed in the spectra of a square-planar Ni(II) complex [45,46].

321 **c. UV-vis spectra and magnetic moment of Mn(II) complex with ligand $C_8H_9ON_3S$ (L^1)**

322 The UV-Vis absorption spectra of the ligand and complex were recorded after dissolving into
323 DMSO solvent at room temperature. There are two absorption bands, assigned to $n-\pi^*$ and
324 $\pi-\pi^*$ transitions, in the electronic spectrum of the ligand. These transitions are also found in
325 the spectra of the complexes, but the ligand to the metallic ions [47]. The electronic spectrum
326 of ligand exhibits three intense absorption peaks at 260 nm, 310 nm and 350nm. The first and
327 second peaks were attributed to benzene $\pi-\pi^*$ and imino $\pi-\pi^*$ transitions and the third peak in
328 the spectra was assigned to $n-\pi^*$ transition. Due to Forbidden transition, several bands were
329 observed in the visible region of Mn(II) complex, and the band at 430 nm is attributed to (d-
330 d) transition of type ${}^6A_1 \rightarrow {}^4T_2$.

331 **d. UV-vis spectra and magnetic moment of Sn(II) complex with ligand $C_8H_9ON_3S$ (L^1)**

332 The electronic absorption spectra of ligand L^1 and its Sn (II) complex in DMSO solution
333 were carried out in the range of 200-800 nm at room temperature. There is a shift of the
334 bands to longer wave length in spectra of complex is a good evidence of complex formation.
335 There were various bands in the ligand spectra assigned to inter ligand and charge transfer of
336 $n-\pi^*$ transitions according to their energies and intensities. Ligand exhibits three intense
337 absorption peaks at 260 nm, 310 nm and 350nm. The first and second peaks were attributed to
338 benzene $\pi-\pi^*$ and imino $\pi-\pi^*$ transitions and the third band in the spectra was assigned to $n-$
339 π^* transition. The complex showed an intense band at 410nm due to the $n-\pi^*$ transition of
340 azomethine chromosphere and the band at 340 nm may be assigned as charge transfer band. It
341 has been reported that the metal is capable of forming $d\pi-\pi\pi^*$ bonds with ligands containing
342 nitrogen as the donor atom. The Sn atom has its 5d orbital completely vacant and hence
343 $Sn \leftarrow N$ bonding can take place by the acceptance of the lone pair of electrons from the
344 azomethine nitrogen of the ligand [48-50].

345

346 **Table-6:** Magnetic moments and electronic spectral data for ligand (L^1) and its metal
347 complexes

Compound	λ_{\max} n.m	Wave number cm^{-1}	μ_{eff} B.M	Assignment
$\text{C}_8\text{H}_9\text{ON}_3\text{S}$	260	38461	-	$\pi \rightarrow \pi^*$
	310	32258		$\pi \rightarrow \pi^*$
	350	38571		$n \rightarrow \pi^*$
$[\text{NiC}_{16}\text{H}_{16}\text{O}_2\text{N}_6\text{S}_2] \cdot \text{H}_2\text{O}$	355	28169	1.469	${}^1\text{A}_{1g} \rightarrow {}^1\text{A}_{2g}$
	380	26315		${}^1\text{A}_{1g} \rightarrow {}^1\text{B}_{1g}$
	420	23809		${}^1\text{A}_{1g} \rightarrow {}^1\text{E}_g$
$[\text{ZnC}_{16}\text{H}_{16}\text{O}_2\text{N}_6\text{S}_2] \cdot 2\text{H}_2\text{O}$	265	37735	0.5197	C.T (M \rightarrow L)
	320	31250		C.T (M \rightarrow L)
	390	25641		C.T (M \rightarrow L)
$[\text{MnC}_{16}\text{H}_{16}\text{O}_2\text{N}_6\text{S}_2] \cdot \text{H}_2\text{O}$	325	30769	2.507	
	380	26315		
	430	23255		${}^6\text{A}_1 \rightarrow {}^4\text{T}_2$

348

349 **e. UV-vis spectra and magnetic moment of Co(II) complex with ligand $\text{C}_{14}\text{H}_{11}\text{O}_3\text{N}$ (L^2)**

350 The magnetic moment and electronic spectra are very effective in the evaluation of results
351 obtained by other methods of structural investigation. Information regarding the geometry of
352 the complex of Co(II) ions was obtained from electronic spectral studies and magnetic
353 moments (Table-7). The electronic spectra of ligand and their metal complexes were recorded
354 in DMSO. Electronic spectrum of ligand shows strong absorption band at 330nm region can
355 be assigned to the $n \rightarrow \pi^*$ transition of the azomethine group of ligand, which slightly shifted
356 to lower frequency in the spectra of the complex, indicating that the azomethine nitrogen
357 atom is involved in coordination to the metal ion. The Co(II) complex was found the
358 magnetic moment 4.0137 B.M which indicated the three unpaired electrons per Co(II) ion
359 attaining an octahedral environment [60]. The electronic spectrum of Co(II) complex shows
360 bands at 264nm and 274nm are assignable to metal-ligand charge transfer band and the band
361 400nm is assignable to ${}^4\text{T}_{1g}(\text{F}) \rightarrow {}^4\text{T}_{1g}(\text{P})$ transition.

362

363 **Table-7:** The electronic spectral data and magnetic moments for ligand (L^2) and it's metal
364 complex

Compound	λ_{\max} n.m	Wave number cm^{-1}	μ_{eff} B.M	Assignment
$\text{C}_{14}\text{H}_{11}\text{O}_3\text{N}$	330	30303	-	$n \rightarrow \pi^*$
$[\text{CoC}_{28}\text{H}_{18}\text{O}_6\text{N}_2] \cdot 2\text{H}_2\text{O}$	264	37878	4.0137	Charge transfer(C.T)
	274	36496		C.T (M \rightarrow L)
	400	25000		${}^4\text{T}_{1g}(\text{F}) \rightarrow {}^4\text{T}_{1g}(\text{P})$

365

366 **f. UV-vis spectra and magnetic moment of Cd(II) complex with ligand $\text{C}_9\text{H}_{11}\text{N}_3\text{OS}$ (L^3)**

367 The electronic spectral data for the ligand and its metal complex recorded in DMSO are
368 summarized in Table-8. There are two absorption bands, assigned to $n \rightarrow \pi^*$ and $\pi \rightarrow \pi^*$
369 transitions, in the electronic spectrum of the ligand. These transitions are also found in the
370 spectra of the complexes, but they are shifted towards lower and higher frequencies,
371 indicating the coordination of the ligand to the metallic ions. The UV spectra of the ligand
372 shows three absorption bands at 280nm, 330nm and 350nm. The first two bands are assigned
373 to $\pi \rightarrow \pi^*$ transitions of azomethine chromospheres and a benzene ring and the third is assigned
374 to $n \rightarrow \pi^*$ transition of a lone pair of electrons of an azomethine nitrogen and an anti-bonding π
375 orbital. The absorption band $n \rightarrow \pi^*$ at 350nm due to an imine group in the ligand, whereas for
376 the Cd(II) complex, the same was observed at 400 nm with weak absorption intensity which
377 indicate the coordination of cadmium with imine group. The cadmium complex show only
378 the charge transfer transition which can be assigned to charge transfer from the ligand to the
379 metal and vice versa, no d-d transition are expected for diamagnetic d^{10} Cd(II) complex. The
380 shifting of ligand absorption in the UV region, in the spectra of the complex confirming the
381 coordination of the ligand to metal like Cd (II) ions.

382

383 **Table-8:** Magnetic moments and electronic spectral data for ligand (L^3) and its Cd(II)
384 Complex

Compound	λ_{\max} n.m	Wave number cm^{-1}	μ_{eff} B.M	Assignment
$\text{C}_9\text{H}_{11}\text{N}_3\text{OS}$	280	35714	-	$\pi \rightarrow \pi^*$
	330	30303		$\pi \rightarrow \pi^*$

	350	28571		$n \rightarrow \pi^*$
[CdC ₁₈ H ₂₂ O ₂ N ₆ S ₂]	295	33898	0.4606	C.T (M→L)
	340	29412		C.T (M→L)
	400	25000		C.T (M→L)

385

386 3.6 Characterization by Thermogravimetric Analysis

387 Thermogravimetric analysis of Zn(II),Ni(II),Mn(II) and Sn(II) complexes of ligand 388 C₈H₉ON₃S (L¹)

389 The thermal decomposition analysis of solid Zn(II), Ni(II), Mn(II) and Sn(II) metal
390 complexes were carried out under nitrogen atmosphere and heating rate was suitably
391 controlled at 30°C min⁻¹ and the weight loss was measured from the ambient temperature up
392 to 800°C. The data from TGA and DTG clearly indicated that the decomposition of the
393 complexes proceed in three or four steps. There were some minor steps and asymmetry of
394 TGA/DTG curves also observed. The weight losses for each complex were calculated within
395 the corresponding temperature ranges. The different thermodynamic parameters are listed in
396 Table-9 and the decomposition curves are shown as supplementary materials.

397 a. For [ZnC₁₆H₁₆O₂N₆S₂].2H₂O Complex

398 The TGA and DTG curve of Zn(II) complex indicated that the complex was decomposed into
399 four main steps. In the first step of decomposition, two molecules of water were lost at the
400 temperature range of 85-110°C (calculated 7.36%, experimental 7.20%). In this temperature
401 range the loss of water molecules indicates that the water molecules are of lattice type
402 [51,52]. In the temperature range 130-335°C (calculated 24.00% and experimental 23.10%),
403 the part of ligand-2CSNH₂ were decomposed at the second step. The other part of the ligand
404 2C₆H₄O⁻ were decomposed in third step at 335-740°C (calculated 37.50%, experimental 32
405 .00%). At above 750°C temperature the complex was decomposed and removed as Zn/ZnO
406 (calculated 31.14%, experimental 37.70%) polluted with few carbon atoms [53].

407 b. For [NiC₁₆H₁₆O₂N₆S₂].H₂O Complex

408 The TGA and DTG curve of Ni(II) complex confirmed that the complex was decomposed
409 into four main steps. The 1st step involves the removal of one molecule of hydrated water
410 (calculated 3.87%, experimental 4.00% weight) at temperature range 80-190°C [54,55]. In the
411 2nd step the part of the ligand 2C₆H₄O⁻ was decomposed at 280-350°C (calculated 39.59%,

412 experimental 34.82% weight). At the 3rd step the fragmentation of coordinated ligand
 413 $2C_2H_4N_3S$ was decomposed from the complex at the temperature range 360-750°C
 414 (calculated 43.90%, experimental 44.20% weight) and above 750°C temperature the complex
 415 was completely decomposed and removed as Ni/NiO (calculated 12.64%, experimental
 416 16.98%).

417 **c. For $[MnC_{16}H_{16}O_2N_6S_2] \cdot H_2O$ Complex**

418 In the case of Mn(II) complex the TGA and DTG curve indicated that the complex was
 419 decomposed into four main steps. At 1st step one molecule of hydrated water was removed at
 420 80-180°C (calculated 3.90%, experimental 4.00%) [54,55]. Then the dehydrated complex was
 421 gradually decomposed and the part of ligand $2C_6H_4O^-$ was removed at the temperature range
 422 180-350°C (calculated 39.92%, experimental 38.10%). The 3rd step involves the
 423 decomposition of the ligand part $2CH_3N_2S$ at the temperature range 350-770°C (calculated
 424 32.54%, experimental 32.22%). At above 770°C temperature finally the complex was
 425 completely decomposed and removed as Mn/MnO (calculated 23.64%, experimental
 426 25.68%).

427 **d. For $[SnC_{16}H_{16}O_2N_6S_2]$ Complex**

428 The Sn(II) complex showed high thermal stability and decomposed above 170 °C, indicating
 429 the absence of any lattice water molecules [69]. This complex was decomposed into four
 430 main steps. At first step the part of ligand $(-2CH_2NS)$ were decomposed at temperature
 431 170-275°C (calculated 23.67%, experimental 22.00%). In 2nd step the decomposition of $(-$
 432 $2CHN-$) moiety was take place at temperature 275-330°C (calculated 12.0%, experimental
 433 10.65 %). The ligand part $(2C_6H_4O^-)$ were decomposed at the 3rd step at temperature range
 434 330-750°C (calculated 36.29%, experimental 36.10 %) and finally the complex was
 435 completely decomposed and removed as Sn/SnO (calculated 28.04%, experimental 31.25%).

436

437 **Table- 9:** Thermal data of Zn(II), Ni(II), Mn(II), Sn(II), Cd(II) and Co(II) complexes.

Complexes	Steps	Temperature Range/ °C	DTG Peak/ °C	TG mass loss% calc./found	Assignments
-----------	-------	-----------------------	--------------	---------------------------	-------------

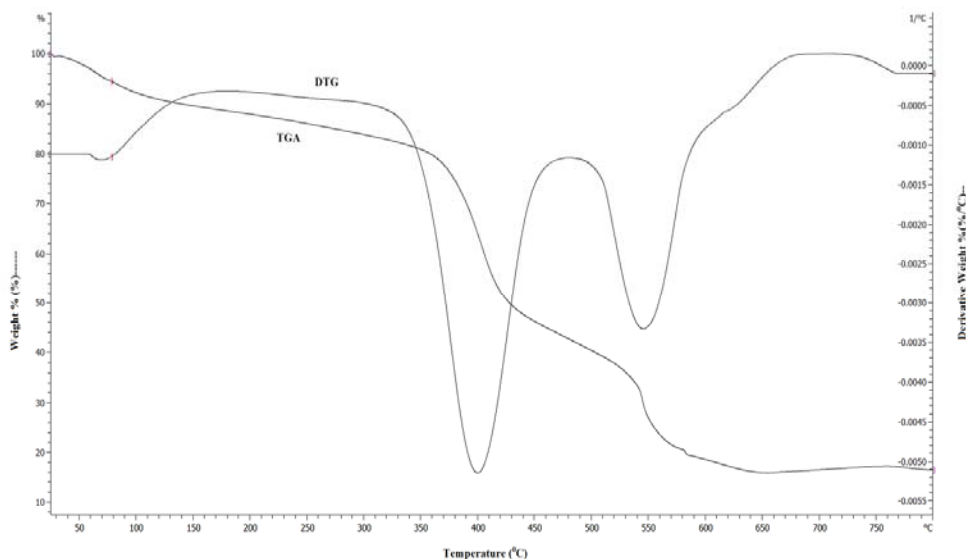
[ZnC ₁₆ H ₁₆ O ₂ N ₆ S ₂].2H ₂ O	1 st	85-110	97	7.36/7.20	2H ₂ O
	2 nd	130-335	278	24.00/23.10	2CSNH ₂
	3 rd	335-740	350	37.50/32.00	2C ₆ H ₄ O-
	4 th	>750		31.14/37.7	Zn/ZnO
[NiC ₁₆ H ₁₆ O ₂ N ₆ S ₂].H ₂ O	1 st	80-190	180	3.87/4.00	H ₂ O
	2 nd	280-350	295	39.59/34.82	2C ₆ H ₄ O ⁻
	3 rd	360-750	382	43.90/44.20	2C ₂ H ₄ N ₃ S
	4 th	>750		12.64/16.98	Ni/NiO
[MnC ₁₆ H ₁₆ O ₂ N ₆ S ₂].H ₂ O	1 st	80-180	118	3.90/4.00	H ₂ O
	2 nd	180-350	290	39.92/38.10	2C ₆ H ₄ O ⁻
	3 rd	350-770		32.54/32.22	2CH ₃ N ₂ S
	4 th	>770		23.64/25.68	Mn/MnO
[SnC ₁₆ H ₁₆ O ₂ N ₆ S ₂]	1 st	170-275	240	23.67/22.00	2CH ₂ NS
	2 nd	275-330	290	12.00/10.65	2CHN-
	3 rd	330-750	370	36.29/36.10	2C ₆ H ₄ O ⁻
	4 th	>750		28.04/31.25	Sn/SnO
[CoC ₂₈ H ₁₈ O ₆ N ₂].2H ₂ O	1 st	40-110	65	6.28/6.32	2H ₂ O
	2 nd	110-480	400	51.31/49.20	2C ₈ H ₅ O ₂ N
	3 rd	480-650	548	32.12/28.80	2C ₆ H ₄ O ⁻
	4 th	>650		10.29/15.72	Co/CoO
[CdC ₁₈ H ₂₂ O ₂ N ₆ S ₂]	1 st	230-455	282	50.53/49.23	2C ₈ H ₈ ON
	2 nd	455-740	570	28.28/27.05	2CH ₃ N ₂ S
	3 rd	>740		21.19/24.00	Cd/CdO

438

439 **Thermogravimetric analysis of Co(II) complex of ligand C₁₄H₁₁O₃N (L²)**

440 TGA was carried out for solid Co(II) metal complex under N₂ flow. The heating rate was
441 suitably controlled at 30°C min⁻¹ and the weight loss was measured from the ambient
442 temperature up to 800°C. The thermogram of complex exhibits three clear cut decomposition
443 stages in (figure-3). The first stage with estimated mass loss of 6.32% (calculated mass loss
444 6.28%) within the temperature range 40–110°C corresponding to the loss of water molecules
445 [56,57]. The second stage occurs at 110–480°C, with a mass loss of 49.20% (calculated
446 51.31%) , corresponding to the loss of 2C₈H₅O₂N parts of the ligand. The third stage of

447 decomposition occurs at the temperature range 480–650°C, with a mass loss of 28.80%
448 (calculated 32.12%), corresponding to the loss of 2C₆H₄O moiety. At above 650°C
449 temperature the complex was completely decomposed and removed as of 15.72% (calculated
450 10.29%). The different TG and DTG data are given in Table-9.



451

452 Figure-3: TGA and DTG curve of [CoC₂₈H₁₈O₆N₂].2H₂O

453

454 **Thermogravimetric analysis of Cd(II) complex of ligand C₉H₁₁N₃OS (L³)**

455 Thermogravimetric analysis of solid Cd(II) metal complex under N₂ flow. The heating rate
456 was suitably controlled at 30°C min⁻¹ and the weight loss was measured from the ambient
457 temperature up to 800°C. The TGA curve of the Cd(II) complex showed no mass loss up to
458 230 °C, indicating the absence of lattice / coordinated water [58,59] and the high thermal
459 stability of the complex. The thermogram of Cd(II) complex is given in Fig.4.24, which
460 shows two stage decomposition pattern. The first stage was exhibited a maximum mass loss
461 of 49.23% (calculated 50.53%) of ligand part (2C₈H₈ON) at 230-455°C. The second stage
462 occurs at 455–740°C, with a mass loss of 27.05% (calculated 28.28%) attributed to the loss
463 of (2CH₃N₂S) moiety. Finally at above 750°C temperature the complex was completely
464 decomposed and removed as Cd/CdO of 24.0% (calculated 21.19%). The different TG and
465 DTG data are given in Table-9.

466 **Antibacterial activity**

467 The prime objective of performing the antibacterial screening is to determine the
 468 susceptibility of the pathogenic microorganism to test the compound which, in turn is used to
 469 selection of the compound as a therapeutic agent. The free Schiff base ligand and their metal
 470 complexes were screened for their antibacterial activity against strains the *Bacillus cereus*
 471 *ATCC25923*, *Streptococcus agelactiae*, *Escherichia coli ATCC 25922*, *Shigella dysenteriae*
 472 The compounds were tested at a concentration of 30 µg/0.01 mL in DMSO solution using the
 473 paper disc diffusion method with Kanamycin as standard. The susceptibility zones were
 474 measured in diameter (mm) and the result are listed in Table-10. The susceptibility zones
 475 were the clear zones around the discs killing the bacteria.

476

477 **Table 10.** Antibacterial activities of the complexes.

Bacterials strains	Zone of inhibition, diameter in mm						
	A (10µg /disc)	B (10µg /disc)	C (10µg /disc)	D (10µg /disc)	E (10µg /disc)	F (10µg /disc)	K (30µg /disc)
Gram positive							
<i>Bacillus cereus</i>	22	10	19	12	11	14	36
<i>Streptococcus agelactiae</i>	19	09	21	08	14	16	35
Gram negative							
<i>Escherichia coli</i>	23	12	24	09	12	18	32
<i>Shigella dysenteriae</i>	09	11	10	12	08	14	36

478

479 Where, A = [C₁₆H₁₆ZnO₂N₆S₂].2H₂O, B = [C₁₆H₁₆NiO₂N₆S₂].H₂O, C = [C₁₆H₁₆MnO₂N₆S₂].H₂O, D =
 480 [C₁₆H₁₆SnO₂N₆S₂], E = [C₂₈H₁₈CoO₆N₂].2H₂O, F = [C₁₈H₂₂CdO₂N₆S₂] and K = Kanamycin

481 **Conclusion**

482 In this paper we have explored the synthesis and coordination Chemistry of Ni(II), Zn(II),
483 Mn(II), Sn(II), Co(II) and Cd(II) ions were synthesized with three different synthesized
484 Schiff base ligands viz (L¹) [2-(2-hydroxybenzylidene)hydrazinecarbothioamide, (L²) [4-((4-
485 hydroxybenzylidene)amino)benzoic acid and (L³) [2-(4-
486 methoxybenzylidene)hydrazinecarbothioamide]. The ligands and metal complexes were
487 characterized by molar conductivity measurement, magnetic susceptibility, Infrared,
488 electronic spectral, thermal analysis and some physical measurements. The overall reactions
489 were monitored by TLC analysis. Molar conductance study have shown that all the
490 complexes were non electrolytic in nature. FTIR studies suggested that Schiff bases act as
491 deprotonated bidentate ligands and metal ions are attached with the ligands-(L¹), (L²) by N, O
492 and ligand-(L³) by N, S coordinating sites during complexation reaction. Magnetic
493 susceptibility data coupled with electronic spectra revealed that [ZnC₁₆H₁₆O₂N₆S₂].2H₂O,
494 [MnC₁₆H₁₆O₂N₆S₂].H₂O, [SnC₁₆H₁₆O₂N₆S₂] and [CdC₁₈H₂₂O₂N₆S₂] complexes have tetrahedral,
495 [NiC₁₆H₁₆O₂N₆S₂].H₂O has square planer and [CoC₂₈H₁₈O₆N₂].2H₂O has octahedral geometry.
496 Thermal analysis (TGA and DTG) data showed the possible degradation pathway of the
497 complexes and also indicated that most of the complexes were thermally stable up to 200⁰C.
498 The Schiff bases and their metal complexes have been found moderate to strong
499 antimicrobial activity.

500

501 REFERENCES

- 502 [1]. Angela Kriza, Lucica Viorica Ababei, Nicoleta Cioatera, Ileana Rău And Nicolae
503 Stănică, Synthesis And Structural Studies Of Complexes Of Cu, Co, Ni And Zn With
504 Isonicotinic Acid Hydrazide And Isonicotinic Acid (1-Naphthylmethylene)Hydrazide,
505 J. Serb. Chem. Soc., 2010;75 (2):229- 242.
- 506 [2]. P. K. Das, N. Panda, N. K. Behera, Synthesis, Characterization and Antimicrobial
507 Activities of Schiff Base Complexes Derived from Isoniazid and Diacetylmonoxime,
508 IJSET – Int. J. of Innovative Sci., Eng. & Tech., 2016;3(1): 42-54.
- 509 [3]. Anil Kumar M R, Shanmukhappa S, Rangaswamy B E, Revanasiddappa M,
510 Synthesis, Characterization, Antimicrobial Activity, Antifungal Activity and DNA
511 Cleavage Studies of Transition Metal Complexes with Schiff Base Ligand, Int. J. of
512 Innovative Sci., Eng. & Tech., 2015;4(2): 60-66.
- 513 [4]. O' Boyle N M, Tenderholt A L & Langer K M, cclib: a library for package-
514 independent computational chemistry algorithms J. Comput. Chem., 2008; 29:839.

- 515 [5]. Saud I. Al-Resayes, Mohammad Shakir, Ambreen Abbasi, Kr. Mohammad Yusuf
516 Amin, Abdul Lateef, Synthesis, spectroscopic characterization and biological
517 activities of N4O2 Schiff base ligand and its metal complexes of Co(II), Ni(II), Cu(II)
518 and Zn(II), *Spectromica Acta Part A*, 2012; 93:86-94.
- 519 [6]. K.D. Karlin, Z. Tyeklar, *Bioinorganic Chemistry of Copper*, Chapman & Hall: New
520 York, 1993;101-109.
- 521 [7]. V. Arun, N. Sridevi, P.P. Robinson, S. Manju, K.K.M. Yusuff, "Ni(II) and Ru(II)
522 Schiff base complexes as catalysts for the reduction of benzene" *J. Mol. Catal. A:*
523 *Chem.*, 2009; 304 (1-2):191-198.
- 524 [8]. K. C. Gupta, A. K. Sutar, Catalytic activities of Schiff base transition metal
525 complexes, *Coord. Chem. Rev.*, 2008; 252 (12-14):1420-1450.
- 526 [9]. R. I. Kureshy, N. H. Khan, S. H. R. Abdi, P. Iyer and S. T. Patel ,Chiral Ru(II) Schiff
527 base complexes catalysed enantio selective epoxidation of styrene derivatives using
528 iodosyl benzene as oxidant II, *J. Mol. Catal.*, 1999;150(1-2):175-183.
- 529 [10]. Saud I. Al-Resayes, Mohammad Shakirb, Ambreen Abbasi, Kr. Mohammad Yusuf
530 Amin, Abdul Lateef, *Spectromica Act.a Part A*, 2012;93:86-94.
- 531 [11]. Rakesh Ranjan and Dhanashree S Hallooman, Synthesis And Characterization Of
532 Co(Ii) And Ni(Ii) Complexes With Schiff Base 2,2-
533 Dimethylpropiophenonethiosemicarbazone, *Int. J. of Res. In Pharm. And Chem.*,
534 2014;4(2):423-426.
- 535 [12]. Angela Kriza, Mariana Loredana Dianu, Nicolae Stănică, Constantin Drăghici, Mona
536 Popoiu, Synthesis and Characterization of Some Transition Metals Complexes with
537 Glyoxalbis- Isonicotinoyl Hydrazone, 2009;60(6):555-560.
- 538 [13]. L. Mitu, A. Kriza, Synthesis and Characterization of Complexes of Mn(II), Co(II),
539 Ni(II) and Cu(II) with an Aroylhydrazone Ligand. *Asian J. Chem.*, 2007;19 (1):658-
540 664.
- 541 [14]. Ljubijankić N., Tešević V., Grgurić-Šipka S., Jadranin M., Begić S., Buljubašić L.,
542 Markotić E., Ljubijankić S., Synthesis and characterization of Ru(III) complexes with
543 thiosemicarbazide-based ligands, 2016;47:1-6.
- 544 [15]. Methak. S. Mohammad, Preparation and Characterization of Some Transition Metal
545 Complexes withSchiff base of thiosemicarbazone, *J. of Kerbala Uni., Scien.* 2010;8
546 (1):8-17 .

- 547 [16]. R.V. Singh, N. Fahmi and M.K. Biyala, Coordination Behavior and Biopotency of N
548 and S/O Donor Ligands with their Palladium(II) and Platinum(II) Complexes, *J. of the*
549 *Ir. Chem. Soc.*, 2005;2(1):40-46.
- 550 [17]. A. M. Vijey, G. Shiny, and V. Vaidhyalingam, Synthesis and antimicrobial activities
551 of 1-(5-substituted-2-oxo indolin-3-ylidene)-4-(substituted pyridin-2-yl)
552 thiosemicarbazide, *Arkivoc (xi)*., 2008;187.
- 553 [18]. Mohammad Asif, A Review On Biological Activities Of Benzimidazole, Oxadiazole
554 And Mannich Base Derivatives Of Benzimidazole-Oxadiazole Merged Compounds,
555 *Int. J. of Cur. Res. in App. Chem. & Chem. Eng.*, 2017;3(1):20-29.
- 556 [19]. M. M. H. Khalil, M. M. Aboaly and R. M. Ramadan, Spectroscopic and
557 electrochemical studies of ruthenium and osmium complexes of salicylideneimine-2-
558 thiophenol Schiff base, *Spectrochimica Acta Part A: Mol. and Bio. Spec.*.,
559 2005;61(1):157-161.
- 560 [20]. P. M. Dahikar, R. M. Kedar, Synthesis, spectral and biological activity of transition
561 metal complexes of substituted benzoinsemicarbazones, *Inter. J. of Appl. or Inn. in*
562 *Engg. & Man. (IJAEM)*, 2013;2(4):8-11.
- 563 [21]. P. Murali Krishna, B. S. Shankara, and N. Shashidhar Reddy, Synthesis,
564 Characterization, and Biological Studies of Binuclear Copper(II) Complexes of (2E)-
565 2-(2-Hydroxy-3-Methoxybenzylidene)-4N-Substituted Hydrazine carbothioamides,
566 Hindawi Publishing Corporation, *International Journal of Inorganic Chemistry*,
567 2013,11pages.
- 568 [22]. Ljiljana S. Vojinović-Ješić, Vukadin M. Leovac, Mirjana M. Lalović, Valerija I.
569 Češljević, Ljiljana S. Jovanović, Marko V. Rodić and Vladimir Divjaković, Transition
570 metal complexes with thiosemicarbazide-based ligands. Part 58. Synthesis, spectral
571 and structural characterization of dioxovanadium(V) complexes with
572 salicylaldehydethiosemicarbazone, *J. Serb. Chem. Soc.* 2011;76 (6):865–877.
- 573 [23]. Monika Tyagi, Sulekh Chandra, Synthesis, characterization and biocidal properties of
574 platinum metal complexes derived from 2,6-diacetylpyridine (bisthiosemicarbazone),
575 *Open Jo. of Inorg. Chem.*., 2012;2:41-48.
- 576 [24]. Vojinović-Ješić Lj. S., Leovac V.M., Lalović M. M., Češljević V.I., Jovanović
577 Lj.S. Rodić M. V. and Divjaković V., Transition metal complexes with
578 thiosemicarbazide-based ligands. Part 58. Synthesis, spectral and structural
579 characterization of dioxovanadium(V) complexes with salicyl aldehyde
580 thiosemicarbazone, *J. Serb. Chem. Soc.*., 2011;76 (6):865–877.

- 581 [25]. Baiu S.H., El-Ajaily M.M. and El-Barasi, Antibacterial Activity of Schiff Base
582 Chelates of Divalent Metal Ions, Asian Journal of Chemistry, (2009);21(1):5-10.
- 583 [26]. Elena Pahontu, Valeriu Fala, Aurelian Gulea, Donald Poirier, Victor Tapcov and
584 Tudor Rosu, Synthesis and Characterization of Some New Cu(II), Ni(II) and Zn(II)
585 Complexes with Salicylidene Thiosemicarbazones: Antibacterial, Antifungal and in
586 Vitro Antileukemia Activity, Molecules, 2013;18:8812-8836.
- 587 [27]. El-Bahnasawy R. M., Sharaf El-Deen L.M., El-Table A.S., Wahba M. A. and El-
588 Monsef. A., Electrical Conductivity Of Salicylaldehyde Thiosemicarbazone and its
589 Pd(II), Cu(II) and Ru(III) Complexes, Eur. Chem. Bull, 2014;3(5):441-446.
- 590 [28]. Md. Saddam Hossain, C.M. Zakaria, M.M.Haque, and Md. Kudrat-E-Zahan, Spectral
591 and thermal characterization with antimicrobial activity on Cr(III) and Sn(II)
592 Complexes containing N,O Donor novel schiff base ligand, Int. J. of Chem. Studies.,
593 2016;4(6):08-11.
- 594 [29]. A. Xavier, P. Gopu, B. Akila, K. Suganya, Synthesis and Characterization of Schiff
595 Base from 3, 5-Di Chloro Salicylaldehyde with 4-Bromoaniline and 4-Aminobenzoic
596 Acid and Its 1st Row Transition Metal Complexes, Int. J. of Inn. Res. & Dev.,
597 2015;4(8):384-396.
- 598 [30]. Manohar V. Lokhande and Mrityunjay R. Choudhary, Some Transitional Metal Ions
599 Complexes With 3-[(E)-(4-Fluorophenyl) Methylidene] Amino} Benzoic Acid And
600 Its Microbial Activity, International Journal of Pharmaceutical Sciences and
601 Research, IJPSR, 2014;5(5):1757-1766.
- 602 [31]. P. Gopu, Dr. A. Xavier, Synthesis and Characterization of 4-(3-bromo-5-chloro-2-
603 hydroxybenzylidene) Benzoic Acid and its Transition Metal Complexes,
604 International Journal of Science and Research (IJSR), 2015;4(8):15-21.
- 605 [32]. Shanker K, Rohini R, Ravinder V and Reddy P M: Ru(II) complexes of N₄ and N₂O₂
606 macrocyclic Schiff base ligands: Their antibacterial and antifungal studies, Spectro
607 chimica Acta A, 2009;73:1205-211.
- 608 [33]. Raju Ashokan, Saravanan Sathishkumar, Ekamparam Akila And Rangappan Rajavel,
609 Synthesis, Characterization and Biological Activity of Schiff Base Metal Complexes
610 Derived from 2, 4-Dihydroxyacetophenone, Chemical Science Transactions, 2017;
611 6(2):277-287.
- 612 [34]. Miguel-Angel Munoz-Hernandes, Michal L. Mckee, Timothy S. Keizer, Burt C.
613 Yearwood and David Atwood, Six-coordinate aluminium cations: characterization,
614 catalysis, and theory, 2002;3.

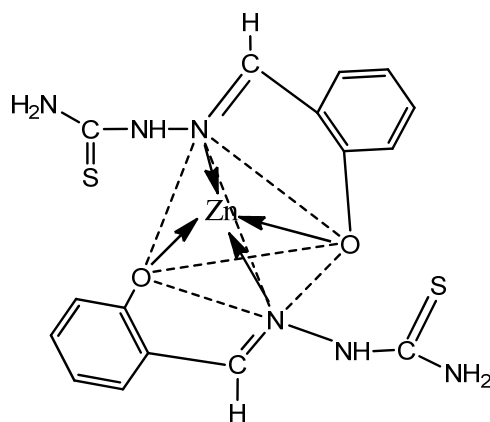
- 615 [35]. K. Nakamoto: Infrared Spectra of Inorganic and Coordination Compounds. John
616 Wiley & Sons, New York, 2nd Edition, 1970.
- 617 [36]. Shanker K B, Rohini M, Ravinder Reddy P and Ho M Y P: Synthesis of Tetraaza
618 Macrocyclic Pd(II) complexes; Antibacterial & Catalytic studies, J.of the Ind. Chem.
619 Soc. 2009, 86.
- 620 [37]. K.P. Satheesh, V. Suryanarayana Rao, Spectrophotometric Method For The
621 Determination Of Trace Amount Of Tungsten (Vi) In Alloy Samples Using 4-
622 Hydroxybenzaldehydethiosemicarbazone, J. of Adv. Scien. Res., 2015; 6(2): 14-17.
- 623 [38]. S. Janarthanan, Y.C. Rajan, P.R. Umarani, D. Jayaraman, D. Premanand and S. Pandi,
624 Synthesis, growth, optical and thermal properties of a new organic crystal
625 semicarbazone of p-anisaldehyde, (SPAS), 2010;3(8):42-47.
- 626 [39]. Ruchi Agarwal, Mohd. Asif Khan and Shamim Ahmad, Schiff base complexes
627 derived from thiosemicarbazone, synthesis characterization and their biological
628 activity , Journal of Chemical and Pharmaceutical Research, 2013;5(10):240-245.
- 629 [40]. Sandra S. Konstantinovi, Blaga C. Radovanovi, IvojinCaki And VesnaVasi, Synthesis
630 and characterization of Co(II), Ni(II), Cu(II) and Zn(II) complexes with 3-
631 salicylidenehydrazono-2-indolinone, J.Serb.Chem.Soc., 2003;68(8-9):641-647.
- 632 [41]. N. K. Gondia, J. Priya, S. K. Sharma, Synthesis and physico-chemical
633 characterization of a Schiff base and its zinc complex, Res Chem Intermed,
634 2017;43:1165-1178.
- 635 [42]. Lotf A. Saghatforoush, Ali Aminkhani, Sohrab Ershad, Ghasem Karimnezhad,
636 Shahriar Ghammamy and Roya Kabiri, Preparation of Zinc (II) and Cadmium (II)
637 Complexes of the Tetradentate Schiff Base Ligand 2-((E)-(2-(2(pyridine-2-yl)-
638 ethylthio)ethylimino)methyl)-4-bromophenol (PytBrsalH), Molecules 2008;13:804-
639 811.
- 640 [43]. Jian-Ning Liu, Bo-Wan Wu, Bing Zhang, Yongchun Liu, Synthesis and
641 Characterization of Metal Complexes of Cu(II), Ni(II), Zn(II), Co(II), Mn(II) and
642 Cd(II) with Tetradentate Schiff Bases, Turk J Chem., 2006;30:41-48.
- 643 [44]. Shayma A. Shaker, Preparation and Spectral Properties of Mixed-Ligand Complexes
644 of VO(IV), Ni(II), Zn(II), Pd(II), Cd(II) and Pb(II) with Dimethylglyoxime and N-
645 Acetyl glycine, E-Journal of Chemistry, 2010;7(S1):S580-S586.
- 646 [45]. Md. Kudrat-E-Zahan, M. S. Islam, and Md. Abul Bashar ,Synthesis, Characteristics,
647 and Antimicrobial Activity of Some Complexes of Mn(II), Fe(III) Co(II), Ni(II),

- 648 Cu(II), and Sb(III) Containing Bidentate Schiff Base of SMDTC, Russian Journal of
649 General Chemistry, 2015;85(3):667–672.
- 650 [46]. Rehab K. Al-Shemary, Ahmed T. Numanand Eman Mutar Atiyah, Synthesis,
651 Characterization And Antimicrobial Evaluation Of Mixed Ligand Complexes Of
652 Manganese(II), Cobalt(II), Copper(II), Nickel(II) And Mercury(II) With 1,10-
653 Phenanthroline And A Bidentate Schiff Base, Eur. Chem. Bull., 2016;5(8):335-338.
- 654 [47]. Iniama, G.E., Olarele, O.S. and Johnson, A, Synthesis, spectral, characterization and
655 antimicrobial activity of manganese (II) and copper (II) complexes of
656 Salicylaldehydephenylhydrazone, Int. J. of Chem. and Appl., 2015;7(1):15-23.
- 657 [48]. Neelofar, Nauman Ali, Shabir Ahmad, Naser M. Abdel-Salam, Riaz Ullah, Robila
658 Nawaz and Sohail Ahmad, Synthesis and evaluation of antioxidant and antimicrobial
659 activities of Schiff base tin (II) complexes, Tropical Journal of Pharmaceutical
660 Research ,2016;15(12):2693-2700.
- 661 [49]. Har Lal Singh and J. B. Singh, Synthesis and Characterization of New Lead(II)and
662 Organotin(IV) Complexes of Schiff Bases Derived from Histidine and Methionine,
663 Hindawi Publishing Corporation, International Journal of Inorganic Chemistry,
664 2012,7pages.
- 665 [50]. Sunita Bhanuka and Har Lal Singh, Spectral, Dft And Antibacterial Studies Of Tin(II)
666 Complexes Of Schiff Bases Derived From Aromatic Aldehyde And Amino Acids,
667 Rasayan J. Chem., 2017; 10(2):673-68.
- 668 [51]. Khalil Abid, Sinann Al-Bayati, Anaam Rasheed, Synthesis, Characterization,
669 Thermal study and Biological Evaluation of Transition Metal Complexes Supported
670 by ONNNO-Pentadentate Schiff Base Ligand, American Journal of Chemistry,
671 2016;6(1):1-7.
- 672 [52]. Allan J. R. and Veitch P. M., The preparation, characterization and thermal analysis
673 studies on complexes of cobalt(II) with 2-, 3-, 4-cyanopyridines, *J. Thermal Anal.*,
674 1983; 27(1): 3-15.
- 675 [53]. Moamen S. Refat, I. M. El-Deen, M. S. El-Garib, and W. Abd El-Fattah,
676 Spectroscopic and Anticancer Studies on New Synthesized Copper(II) and
677 Manganese(II) Complexes with 1,2,4- Triazines Thiosemicarbazide1, Russian J. of
678 Gen. Chem., 2015;85(3): 692–707.
- 679 [54]. Md. Saddam Hossain, Md. Ashraful Islam, C. M. Zakaria, M. M. Haque, Md. Abdul
680 Mannan, Md. Kudrat-E-Zahan, Synthesis, Spectral and Thermal Characterization with
681 Antimicrobial Studies on Mn(II), Fe(II), Co(II) and Sn(II) Complexes of Tridentate

- 682 N,O Coordinating Novel Schiff Base Ligand” J. Chem. Bio. Phy. Sci. Sec. A., 2016;6
683 (1):041-052.
- 684 [55]. M. R. Islam, J. A. Shampa, M. Kudrat-E-Zahan, M. M. Haque, Y. Reza, Investigation
685 on Spectroscopic, Thermal and Antimicrobial Activity of Newly Synthesized
686 Binuclear Cr(III) Metal Ion Complex , J. Sci. Res., 2016;8 (2):181-189.
- 687 [56]. Sayed M. Abdallah, M.A. Zayed, Gehad G. Mohamed, Synthesis and spectroscopic
688 characterization of new tetradentate Schiff base and its coordination compounds of
689 NOON donor atoms and their antibacterial and antifungal activity, Arabian J. of
690 Chem., 2010; 3:103–113.
- 691 [57]. Samir Alghool. Mononuclear complexes based on reduced Schiff base derived fromL-
692 methionine, synthesis, characterization, thermal and in vitro antimicrobial studies, J
693 Therm Anal Calorim, 2015; 12: 1309–1319.
- 694 [58]. Achut S. Munde, Amarnath N. Jagdale, Sarika M. Jadhav And Trimbak K.
695 Chondhekar, Synthesis, characterization and thermal study of some transition metal
696 complexes of an asymmetrical tetradentate Schiff base ligand, J. Serb. Chem. Soc.,
697 2010;75(3):349–359.
- 698 [59]. A.S. Munde, V. A. Shelke, S. M. Jadhav, A. S. Kirdant, S. R. Vaidya, S. G.
699 Shankarwar, and T. K. Chondhekar, Synthesis, Characterization and Antimicrobial
700 Activities of some Transition Metal Complexes of Biologically Active Asymmetrical
701 Tetradentate Ligands, Adv. Appl. Sci. Res., 2012; 3(1):175-182.

702

703 **Supplementary Materials**

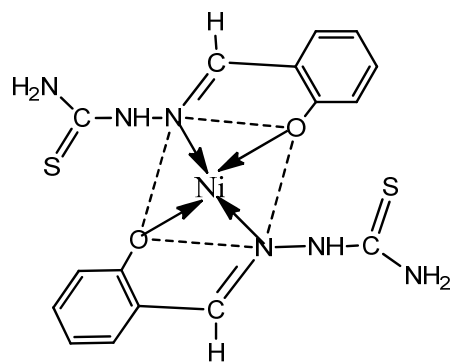


704

705

Figure: Structure of $[C_{16}H_{16}ZnO_2N_6S_2]$

706

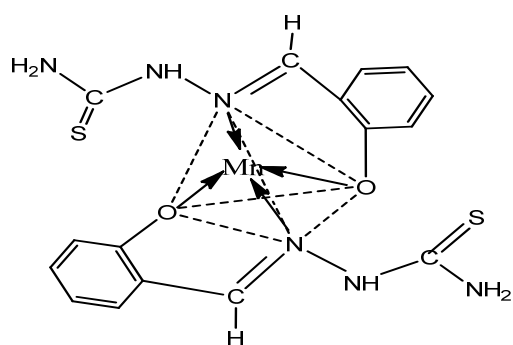


707

708

Figure: Structure of $[C_{16}H_{16}NiO_2N_6S_2]$

709

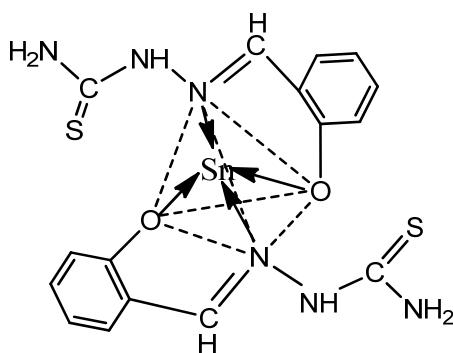


710

711

Figure: Structure of $[C_{16}H_{16}MnO_2N_6S_2]$

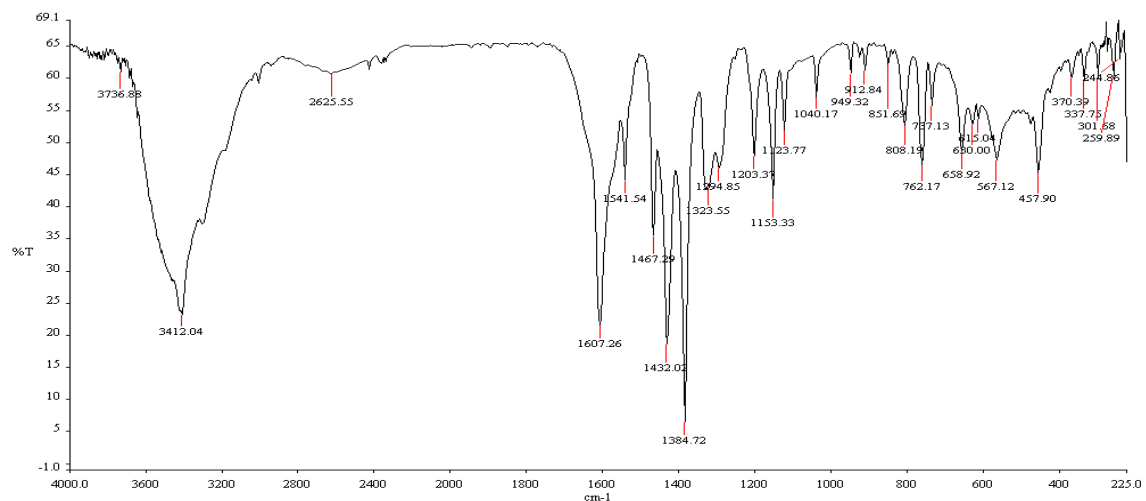
712



713

714

Figure: Structure of $[C_{16}H_{16}SnO_2N_6S_2]$



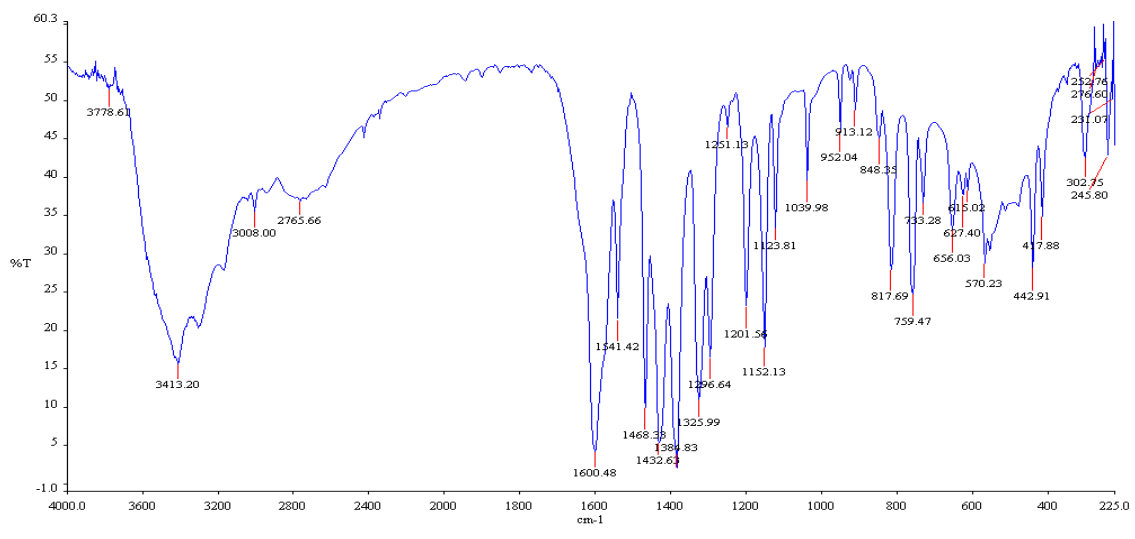
715

Figure: IR spectra of $[\text{NiC}_{16}\text{H}_{16}\text{O}_2\text{N}_6\text{S}_2]\cdot\text{H}_2\text{O}$

716

717

718

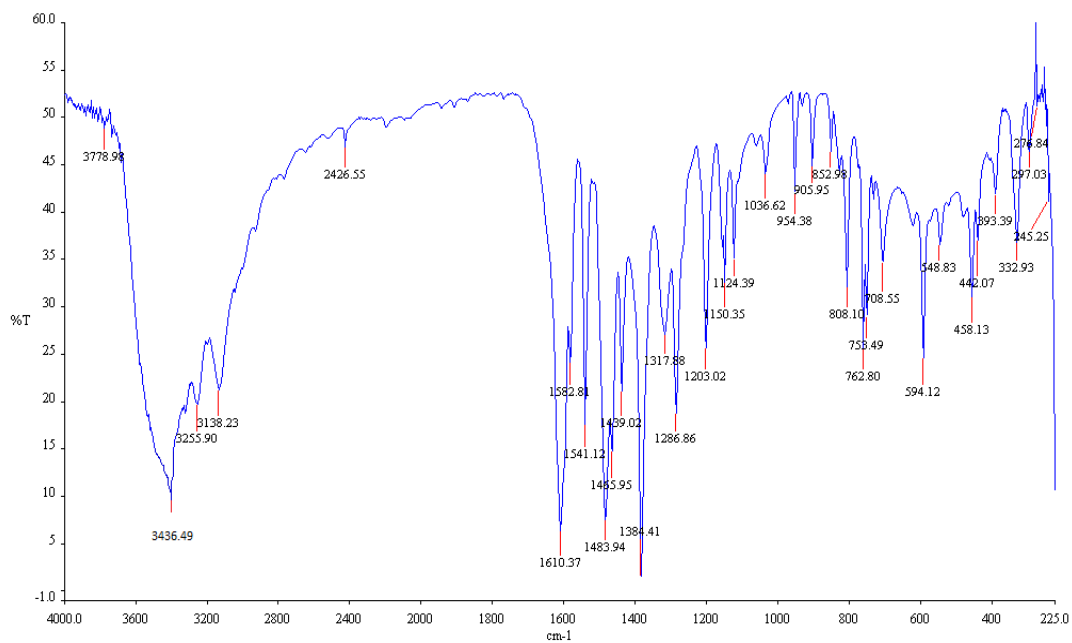


719

Figure: IR spectra of $[\text{MnC}_{16}\text{H}_{16}\text{O}_2\text{N}_6\text{S}_2]\cdot\text{H}_2\text{O}$

720

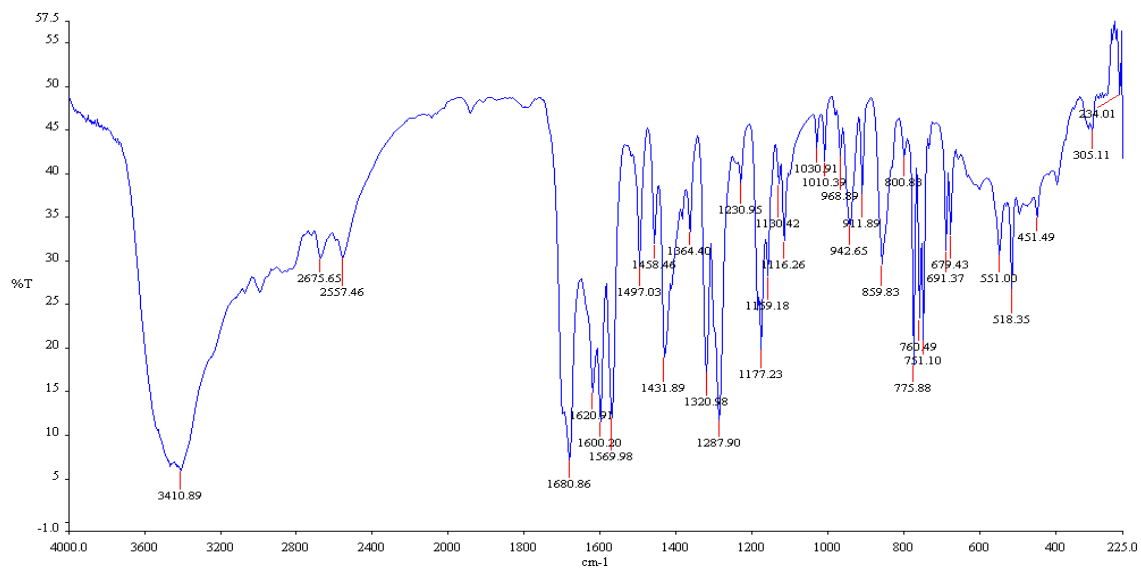
721



722

723

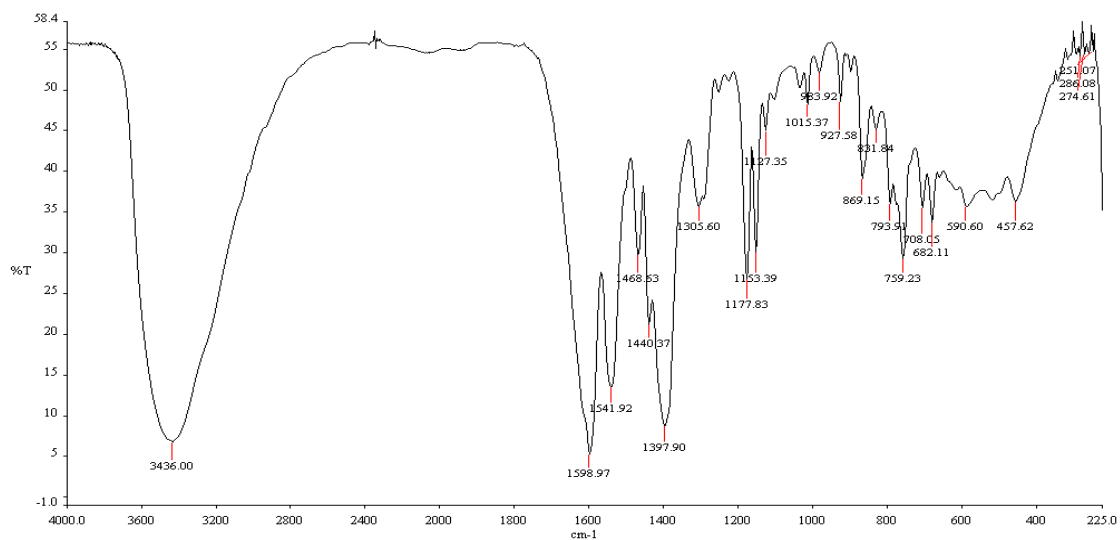
Figure: IR spectra of [SnC₁₆H₁₆O₂N₆S₂]



724

725

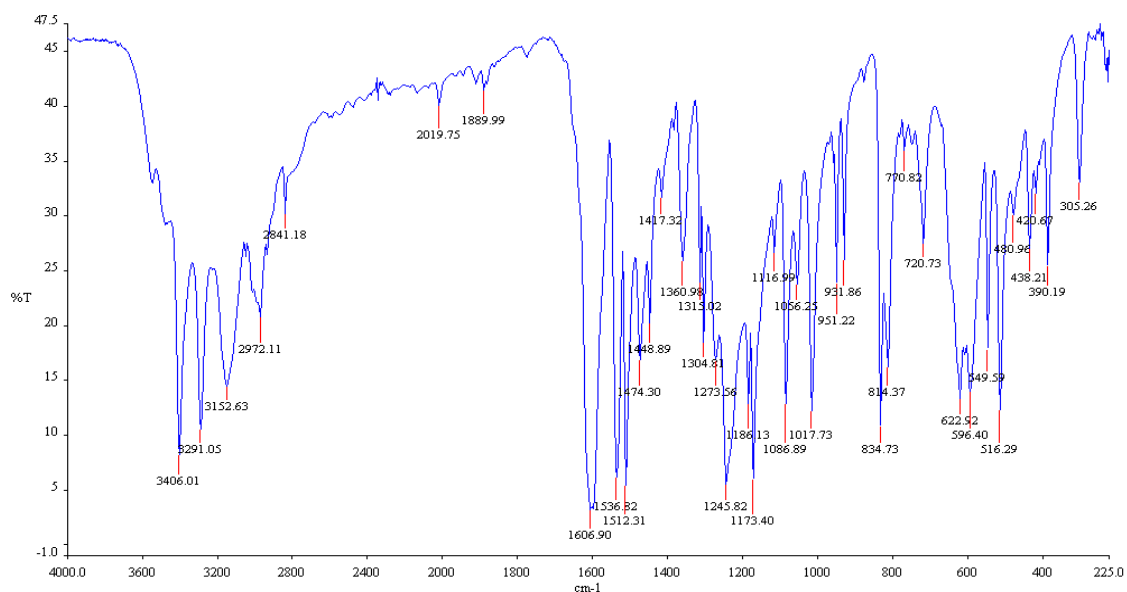
Figure: IR Spectra of 4-((hydroxybenzylidene)amino)benzoic acid ligand(L²)



726

727

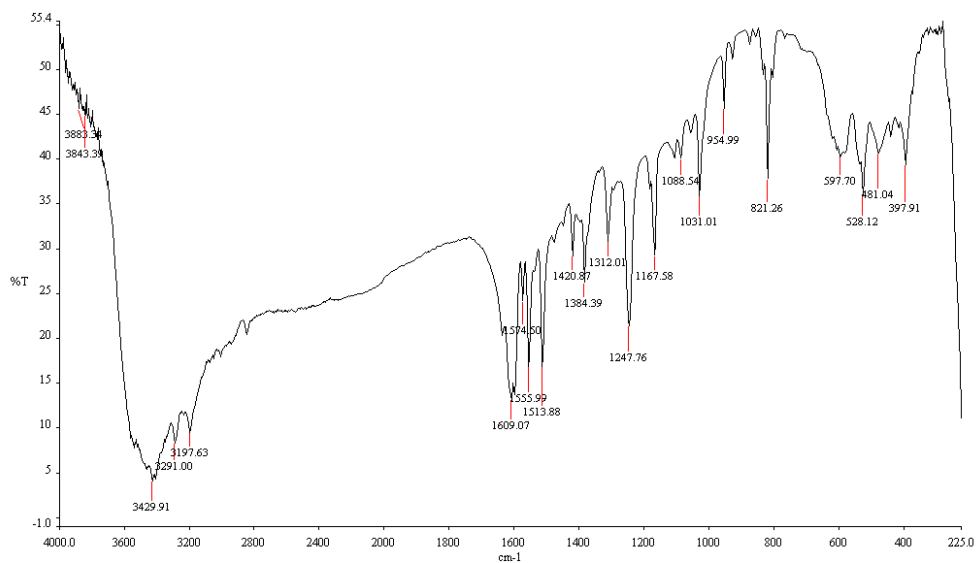
Figure: IR Spectra of $[CoC_{28}H_{18}O_6N_2] \cdot 2H_2O$ with ligand (L^2)



728

729

Figure: IR Spectra of Schiff base ligand $C_9H_{11}N_3OS$ (L^3)

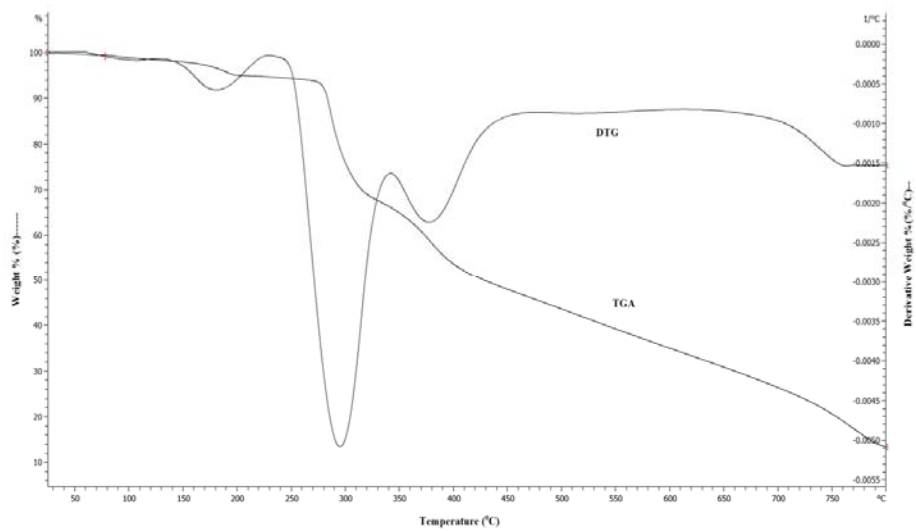


730

731

Figure: IR Spectra of $[\text{CdC}_{18}\text{H}_{22}\text{O}_2\text{N}_6\text{S}_2]$

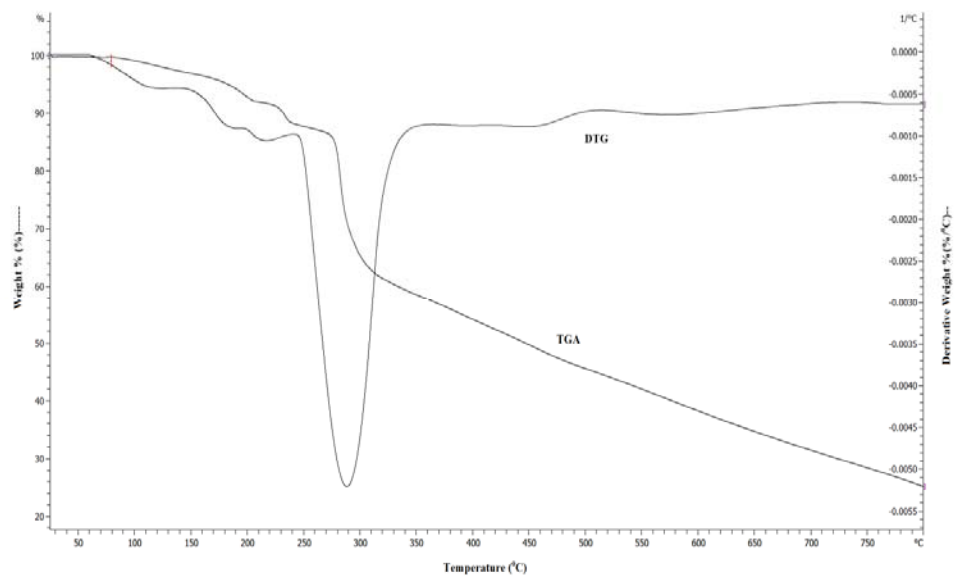
732



733

734

Figure: TGA and DTG curve of $[\text{NiC}_{16}\text{H}_{16}\text{O}_2\text{N}_6\text{S}_2] \cdot \text{H}_2\text{O}$

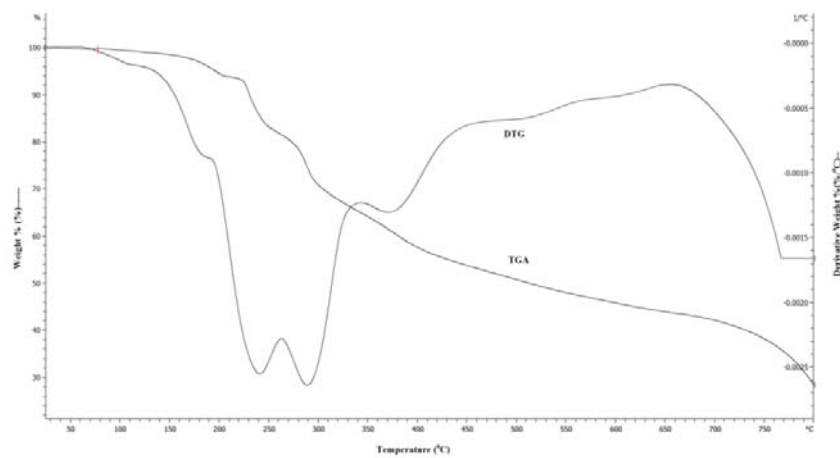


735

Figure: TGA and DTG curve of $[\text{MnC}_{16}\text{H}_{16}\text{O}_2\text{N}_6\text{S}_2]\cdot\text{H}_2\text{O}$

736

737

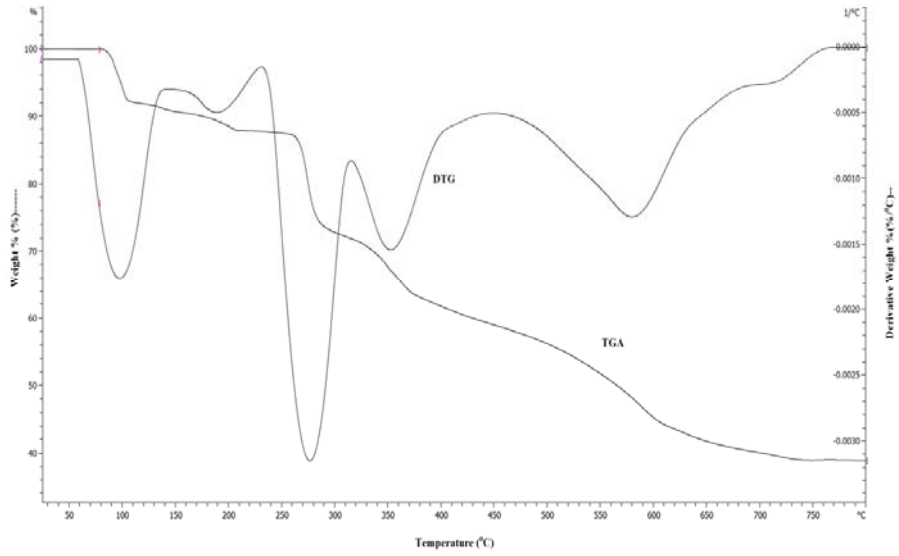


738

Figure: TGA and DTG curve of $[\text{SnC}_{16}\text{H}_{16}\text{O}_2\text{N}_6\text{S}_2]$

739

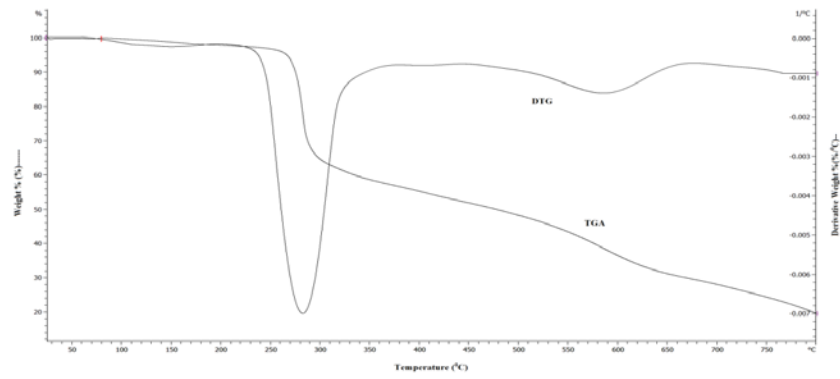
740



741

742

Figure: TGA and DTG curve of $[\text{ZnC}_{16}\text{H}_{16}\text{O}_2\text{N}_6\text{S}_2] \cdot 2\text{H}_2\text{O}$



743

744

Figure: TGA and DTG curve of $[\text{CdC}_{18}\text{H}_{22}\text{O}_2\text{N}_6\text{S}_2]$

745